THESIS

SEISMIC PERFORMANCE OF SKEWED AND CURVED RC BRIDGES

Submitted by

Thomas Wilson

Department of Civil and Environmental Engineering

In partial fulfillment of the requirements

For the Degree of Master of Science

Colorado State University

Fort Collins, Colorado

Summer 2013

Master's Committee:

Advisor: Suren Chen
Co-Advisor: Hussam Mahmoud

Kelly Strong
Joshua Johnson

ABSTRACT

SEISMIC PERFORMANCE OF SKEWED AND CURVED RC BRIDGES

Explicit knowledge of the behavioral response of complex reinforced concrete (RC) highway bridges to seismic events is essential to designing safe transportation systems. In the past, a number of skewed and curved highway bridges have experienced damage or suffered collapse due to earthquakes; and have most recently been observed during the Chile earthquake in 2010. Yet, there is very limited information on the combined effects of skew and curvature on the seismic response of RC bridges, and in particular identifying critical vulnerabilities to localized failures or system collapse. Recent research has also shown that the vertical component of earthquake ground motion, previously not considered, may have significant bearing on the response of highway bridges, particularly in near-fault regions. This study is comprised of two parts, including an examination of skewed and curved RC bridges of various configurations representative of a low seismic region, and an evaluation of the effect of vertical ground motion on complex geometry bridges in a moderate, near-fault, seismic region. Detailed numerical models are developed for various configurations of skew and curvature, and subjected to earthquake ground motion using nonlinear time-history analysis.

In part one, detailed finite element models are developed and analyzed for eight bridge configurations of various degrees of skew and curvature, with consistent structural and geometric components. The bridge designs and earthquake hazard level are characteristic of the Mountain West region where the seismic risk is typically classified as low to moderate. Nonlinear time-history analysis is conducted on each bridge configuration for seven sets of earthquake records scaled to a site location in Denver, Colorado. The effects of earthquake input loading direction

and abutment support condition, including integral and bearing supports, are also considered. The results show significant impacts on the seismic performance due to the effects of skew and curvature with stacking effects observed in the combined geometries. Insights on the complexities of curvature, skew, loading direction and support condition are made, which may lend themselves to more informed design decisions in the future.

Part two of this study presents an assessment of the effect of vertical ground motion on horizontally skewed and curved highway bridges in moderate-to-high seismic regions. A numerical model of a skewed and curved, three-span bridge located in Tacoma, Washington is subjected to a suite of ground motions using non-linear time-history analysis. The ground motions selected represent a range of near-fault records with varying characteristics such as site condition, fault distance, and vertical-to-horizontal acceleration component ratios. The scenario developed characterizes the behavior of a bridge with a short fundamental period of vibration in a moderate seismic zone, where vertical ground motion effects may be applicable yet not considered by structural code. The results of the numerical simulations depict a significant impact from vertical ground motion in the substructure and superstructure, including responses typically not documented in existing studies. The implications of the results for structural designers may be to reconsider the current design approach involving vertical ground motion, particularly with shorter period bridges involving configurations of skew and curvature.

TABLE OF CONTENTS

LIST OF FIGURES

LIST OF TABLES

Chapter 1: Introduction

1.1 Background

Earthquakes are a present-day hazard to the expanding infrastructure in the United States and are currently responsible for approximately $5.3 billion in annual economic losses (FEMA 366, 2008). An earthquake can cause damage to, and in cases collapse of buildings, civil structures, railways, and bridges. In the case of a severely damaged or collapsed bridge the consequences can be substantial in terms of financial losses due to cost of repair or replacement of the bridge, in addition to the socioeconomic losses through the value of lost time to the public by a longer work commute. Bridges are typically designed for life loss prevention under large seismic demand, which requires a design that prevents structural collapse under large cyclic demands. The response of bridges to earthquake ground motion however is difficult to predict and often requires rigorous analyses. Therefore it may be advantageous to identify critical vulnerabilities and behavioral trends such that seismic based bridge design can be better focused.

Structural codes typically classify bridges into seismic zones based on their location, the seismic history of the area, and the known exposure to active faults. In the central United States (U.S) the tectonic setting is primarily classified by intra-plate tectonics, which generates earthquakes of typically smaller magnitude over longer periods of time. States in the central U.S. are typically classified as low seismic regions and incorporate little to no seismic design or analyses into their bridge practices. Coastal states like California and Washington, which frequently experience moderate-to-large magnitude earthquakes, are classified as high seismic regions. The seismic activity in states like California stems from active inter-plate tectonic interaction, which can result in frequent and sometimes large magnitude earthquakes.

Most states, independent of seismic hazard level, utilize the American Association of State Highway and Transportation Officials (AASHTO) LRFD Bridge Design Specifications and the AASHTO Guide Specifications for LRFD Seismic Bridge Design. Each code presents a method of design against earthquakes following force-based and displacement-based design practices, respectively. California has developed its own seismic design guidelines in the California Design Criteria (SDC 2006), which adopts an independent performance-based procedure. All design codes utilize simplified analysis procedures however, based on existing knowledge, analysis and testing, levels of seismic risk, and geometric variations.

Skewed and curved highway bridges are frequently used in transportation systems because of their ability to conform to existing layouts, and facilitate easy access or egress from complex intersections, often useful in dense urban areas. Although the offset angle of skewed bridges may present advantages to the transportation layout, a more complex structural response to an earthquake can occur, leading to higher induced stresses and unforeseen failure modes. Examples of these kind of responses and failures of skewed reinforced concrete bridges have been observed following the earthquakes in Costa Rica (1991), Northridge (1994) and more recently in Chile (2010). Similar to skewed bridges, the configuration of curved bridges induces a structural response to earthquakes that is complex and difficult to predict. Notable failures of curved bridges have occurred in the past calling for further research on the dynamic response under seismic loads, yet existing studies have been focused almost entirely on steel bridges. The research in both areas is also not comprehensive. There are a large number of bridges across the country that incorporate both curvature and skew, and there is very limited information on the interaction between the two geometries and what the overall implications would be during an earthquake.

Until the early 1990's, not much was known about vertical ground motion and it was not generally incorporated into analysis or design of civil structures. Since then studies have shown that in moderate-high seismic regions, where a structure may be at a close proximity to the source of an earthquake, vertical ground motion may influence the response and should be considered. Seismic ground motion is typically discretized into three directions including two perpendicular horizontal components and a singular vertical component. In the analysis of bridges, the applied earthquake is generally only considered in two orthogonal directions in the horizontal plane. This approach typically represents the most conservative scenario when considering just horizontal ground motion and the angle of the incidence of the earthquake. In the AASHTO codes, vertical ground motion is not addressed in code provisions (AASHTO, 2009). The Caltrans Seismic Design Criteria (SDC, 2006) is one of the few codes that have accounted for the vertical ground motion component by means of applying an equivalent static loading. In the research conducted in the past decade, studies have shown, however, that for particular cases of regular geometry bridges, all these approaches can be non-conservative.

1.2 Thesis Layout

The following study is partitioned into two major contributions, targeted at providing a review of the seismic performance of skewed and curved RC highway bridges. Chapter 2 provides a summary of existing research on the topics discussed in this study. This includes a review of the existing knowledge on the seismic activity of the Colorado region, the seismic performance of skewed and curved bridges, vertical ground motion, and a summary of modeling techniques and analytical methods. Chapters 3 and 4 are formatted as independent journal papers, which have been submitted and are being prepared for submission to journals respectively. Chapter 3 evaluates the seismic performance of skewed and curved reinforced

concrete bridges in mountainous states. The study is focused in Denver, Colorado and utilizes typical bridge specifications provided by the Colorado Department of Transportation, as to provide a viable scenario. Chapter 4 evaluates the effects of vertical ground motion on a skewed and curved bridge. Vertical ground motion is most applicable in moderate-high seismic regions where structures are often built in close proximity to a potential earthquake source. The earthquake scenarios in this study are carried out on a bridge in Tacoma, Washington, which is considered a moderate-high seismic zone.

1.3 Objective

The objective of this study is to evaluate the combined effects of skew and curvature on the seismic performance of reinforced concrete bridges. Chapter 3 evaluates the impact of skew and curvature on the seismic performance of RC bridges, independently and conjointly, in a low seismic region. Past studies have shown that both structural configurations yield individual vulnerabilities to ground motions; however the response of the combined systems to moderate earthquakes has not been well documented. Through detailed finite element models and utilizing various analytical tools for imposing seismic demand, the dynamic behavior of bridges of various skewed and curved configurations are studied and evaluated. Insights will be made on the complexities of curvature and skew, as well as considerations to design decisions such as loading direction and support condition. In this manner, the conclusions on conditional parameters may lend themselves to more informed design decisions in the future.

The objective of the research conducted in Chapter 4 is to investigate the effects of vertical ground motion on geometrically complex bridges. A prestressed concrete skewed, curved, box-girder bridge in Tacoma, Washington presents a realistic and viable case for investigating effects of vertical ground motion. An earthquake set with varying characteristic contributions of vertical

ground motion is used such that conclusions can be drawn on both the bridge response and the characteristics of the ground motion.

The overall objective of this study is to assess the seismic performance of skewed and curved bridges, with varying structural components and hazard scenarios. The analyses conducted can be beneficial to researchers and structural designers alike, as it provides a continuation to an expanding knowledge base on the response of geometrically complex bridges.

1.4 References

AASHTO. (2009). *AASHTO Guide Specifications for LRFD Seismic Bridge Design* (1st ed.). Washington, DC: AASHTO.

Berman, E. (2008). *Estimated Annualized Earthquake Losses for the United States*. *FEMA 366*.

California Department of Transportation. (2006). Caltrans Seismic Design Criteria, (1.6), 161.

Kawashima, K., Unjoh, S., & Hoshikuma, J. (2010). Damage of transportation facility due to 2010 Chile Earthquake.

Maragakis, E. (1984). *A model for the rigid body motions of skew bridges*. Pasadena, California.

Moehle, J., & Eberhard, M. (2000). *Earthquake damage to bridges*. (W.-F. Chen & L. Duan, Eds.)*Bridge Engineering Handbook*. CRC Press, 2000.

Chapter 2: Literature Review

2.1 Introduction

The work conducted in this thesis addresses the impact of skew and curvature on highway bridges in low seismic region (Chapter 3); and the impact of vertical ground motion in bridges in high seismic regions (Chapter 4). The following literary review summarizes general structural code provisions, existing research on geometrically irregular bridge and vertical ground motion, and includes typical analytical assessment and numerical modeling methods used for seismic bridge analyses.

Most states, with the exclusion of California, utilize the AASHTO specifications for bridge design against seismic events. There are currently two structural codes employed by AASHTO for design of bridges that have specific guidelines per region, hazard exposure, structural classification, and site condition. The AASHTO LRFD Bridge Design Specifications and AASHTO Guide for LRFD Bridge Design Specifications (hereon referred to as the Bridge Spec. and Guide Spec. respectively) present two independent methods of force-based design and ductility-based design respectively. Following the hazard assessment criteria developed in the AASHTO codes, bridge design against earthquakes in Colorado includes basic provisions, but does not require any specific seismic analysis. Straight and simple-span bridges make up a predominant proportion of bridges in Colorado, along with bridges that incorporate skew and curvature as they facilitate an effective option for more complex traffic intersections. Although the response to regular loading of complex bridges has been studied, the dynamic response of bridges incorporating both skew and curvature has not been thoroughly investigated.

Earthquake ground motion can be subdivided into three primary directional components. Two of these components are in the horizontal plane, at directions perpendicular to each other.

The third component is the vertical, generally not considered in design. In regions of low seismicity, or where the location of the structure is at a large enough distance from active faults, the vertical component attenuates, thus using the two horizontal components can be deemed appropriate design. For structures in moderate-to-high seismic regions, and near proximity to active faults, the vertical component of ground motion is much more prominent and can be underestimated by code provisions. A number of research studies, discussed later, have shown the importance of considering vertical ground motion and its contribution to particular modes of failures of regular reinforced concrete bridges. The interaction between vertical ground motion and regular geometry bridges has been well documented, although scenarios involving geometric attributes such as skew and curvature that are known to also have significant bearing on the structural response have not yet been assessed.

The most current methods for analysis of bridges under seismic loading include pushover analysis, modal analysis, response spectrum analysis and time-history analysis. These analysis methods are referenced in the AASHTO codes for imposing seismic demand on bridge structures. The following literary review summarizes the conducted research on the exposed hazard and seismic history of Colorado, as well as the method of design and analysis per the two AASHTO codes. It also discusses analytical studies conducted on the effects of skew and curvature on highway bridges, vertical ground motion, in addition to a review of current numerical modeling and analytical methods.

2.2 Hazard Characteristics and Seismic Activity in Colorado

Earthquakes pose a present threat to society and infrastructure in the United States and around the world. Improper design of infrastructure against seismic events can result in collapse or extensive damage to roads, bridges, buildings, and utility lines. Colorado, like many other

states across the United States is recognized by AASHTO structural code as a low seismic hazard region. AASHTO codes utilize United States Geological Survey (USGS) hazard maps (Fig. 2.1) that assign representative peak horizontal accelerations based on geography and tectonic activity across the United States. Based on the assigned peak acceleration and the seismic category that the location falls into, the level of seismic analysis required is assessed. Colorado is classified state wide as a seismic class A and does not require any specific seismic analysis according to the AASHTO LRFD Bridge Design Specifications and Guide Specifications.

Figure 2.1 Seismic Hazard Maps for AASHTO Guide Specifications, Peak Horizontal Acceleration (7% in 75-year) (2009)

The seismicity of Colorado is still uncertain according to seismologists and the state may be more active than currently presumed (Charlie et al. 2006; Sheehan et al. 2003). Generally Colorado is thought as a low seismic region; it has a low number of previously recorded seismic events in the area and spans a large distance from major inter-plate fault lines such as those present in California. Inter-plate faults are characterized by the junction and interaction of two tectonic plates. Present at these junctions are large tectonic forces that result in fracturing of the lithosphere-asthenosphere complex generating frequent and larger magnitude earthquakes. The

seismic activity present in Colorado is rather characterized by intra-plate tectonic interaction. The occurrence of intra-plate earthquakes is attributed to internal fractures of the lithosphere on the tectonic plate. The interaction is complex, and difficult to predict. The generation of earthquakes across the lithosphere may be attributed to anomalies in temperature, strength or by the nature of the geological site conditions. Colorado has 58 mountain peaks of elevation larger than 14,000 feet, apparent Neogene and active quaternary deformation, and the second to largest heat flow anomaly, which all point towards an active tectonic area (Charlie et al., 2002). In addition, there are ninety-two potentially active quaternary faults documented. Of the ninety two faults, thirteen have a maximum credible earthquake (MCE) of higher than 6.25 M_L (Fig. 2.2) on the Richter Scale (Widmann et al. 1998). The maximum credible earthquake scale is based on a 2500 year return period, and is utilized to assess the highest magnitude earthquake a fault line may produce and the largest seismic event a region may be exposed to. In light of the inherent impracticalities of design and construction of bridges using the MCE, the design based earthquake (DBE) is utilized for most the design of most bridges and represents a 1000 year return period.

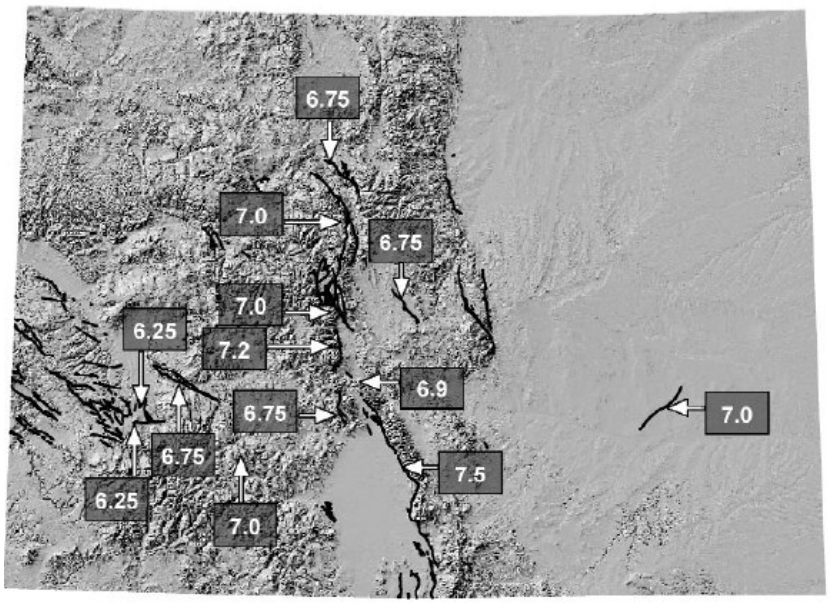

Figure 2.2 (Matthews, 2002) Quaternary Fault Lines with Assigned Maximum Credible Earthquake Magnitudes for the State of Colorado

The focal point of recorded seismic activity has been centered just west of the Rocky Mountain Front Range and in Southern Colorado near Trinidad. The largest earthquake to date was recorded on November 7, 1882 and measured a magnitude of 6.6 ± 0.6 M_L on the Richter Scale (Spence et al. 1996; Kirkham & Rogers 2000). The ground motion was observed throughout several neighboring states, as shown in Figure 2.3, and is estimated to have affected an area of 850,000 km^2 (Spence 1999). The unified estimate on the Modified Mercalli Intensity (MMI) scale was assessed by seismologists at an intensity of VII (R. Kirkham 1986). Colorado is one of only fourteen states across the country to have documented an earthquake of magnitude 6.0 or greater (Stover & Coffman 1993).

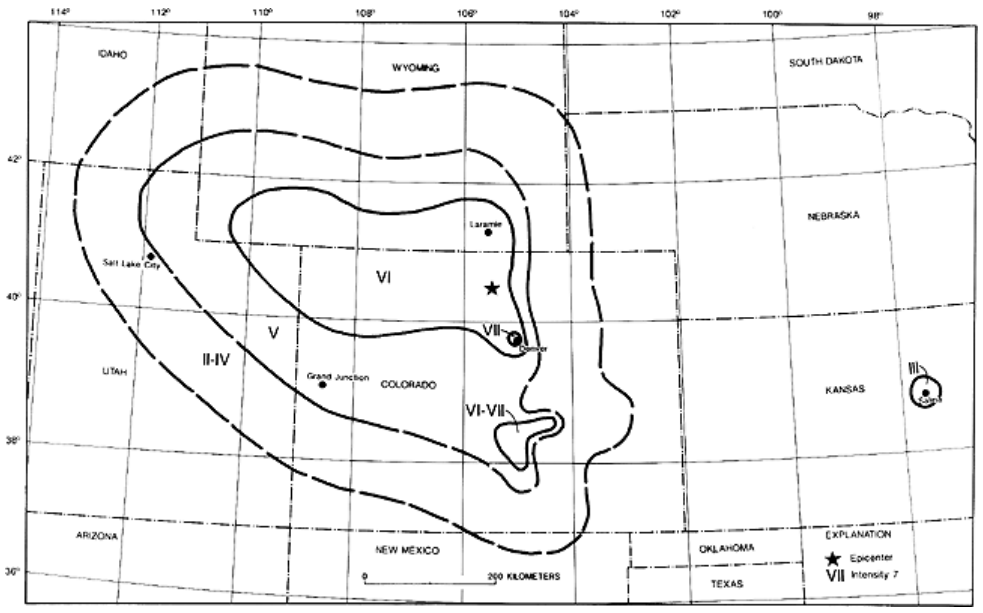

Figure 2.3 (Stover & Coffman, 1993) Isoseismal Map for November 7th, 1882 Earthquake in Colorado

A total of 570 earthquakes have also been recorded from 1870 to 2005 of Moment Magnitude (M_W) 2.0 or higher. Of these 570 earthquakes, 82 earthquakes have been recorded at a MMI scale of V or higher. Colorado's highest probability for a seismic event measure using the MCE scale, is estimated at magnitude 7.5 M_L on the Richter scale (Kirkham & Rogers, 1985). According to Charlie et al. (2006), data collected from independent earthquakes yields a mean recurrence interval of 420 years for an earthquake of magnitude 6.5 M_L or larger. Applying a Gutenberg-Richter magnitude-recurrence relation developed by Charlie et al. (2002) yields that a magnitude 6.6 M_L or larger earthquake will have a corresponding return period of 500 years. Applying the same relationship, a 1000-year return period corresponds to a 7.0 M_L event, and a 2500-year return period corresponds to a 7.5 M_L event. In comparison, by current AASHTO design criteria, Colorado falls into a Seismic Design Category A for a 1000 year return period, which dictates that seismic design is not required. Comparing the estimated earthquake

magnitudes by seismologists and AASHTO seismic hazard maps for comparable return periods, there appears to be a significantly larger estimated hazard by seismologists than what is estimated by AASHTO structural code.

2.3 Structural Code Design Approach

Prior to the magnitude 6.6 M_w earthquake that struck the San Fernando Valley in the state of California in 1971, guidelines on seismic design were fairly rudimentary. A small fraction of the dead load from the structure was used to estimate the lateral seismic loads, based on which the members of the structural system were designed. Following the earthquake in 1971, a group of experts in the field of seismology and structural engineering wrote a document, which was published in 1981 by the Applied Technology Council (ATC), titled "Seismic Design Guidelines for Highway Bridges" (ATC-6 1981). ATC-6 was later adopted as the guide for seismic design in the AASHTO Standard Specification Division 1-A. Since then, further development and updates have followed in the AASHTO LRFD Bridge Design Specification (AASHTO 2007). In 2007, AASHTO introduced the LRFD Guide Specifications for Seismic Design of Highway Bridges in addition to updates to the existing specifications. The updates to the existing specifications and the introduction of the Guide Specifications were a shift towards life safety performance. Life safety performance dictated that a bridge would be designed such that it has low probability of collapse, although it may sustain significant amounts of damage such that partial or complete rehabilitation may be required following a high magnitude seismic event. Supplementing this change was an increase in the return period of the design event from 475 years to 1000 years, which was included in both specifications.

The AASHTO LRFD Bridge Design Specifications is based on traditional force-based seismic design and relies on the capacity of the individual structural members to perform in the

inelastic range, although the seismic loads are determined through elastic analysis. To determine the level of analysis required, the AASHTO Bridge Specifications differentiates a bridge into four Seismic Zones (SZ) partitioned by acceleration coefficient ranges. The acceleration coefficients are devised from seismic hazard maps developed by the USGS. Based on the seismic zone and bridge classification, the minimum analysis requirements are determined. For SZ one, applicable to Colorado, no seismic analyses are required, however a small fraction of the vertical load is applied horizontally to determine the required connection strength and ensure that minimum requirements for deck unseating are met. In contrast to critical bridges in SZ four, response-time history method is the minimum analysis requirement and a series of far more detailed performance criteria need to be met. The general method for analyses requires developing a unique response spectrum using spectral maps and site-specific soil classifications. Following calculation of elastic force based effects with the response spectrum, a response modification factor (Fig. 2.4) is utilized to scale down seismic forces in recognition of the fact that it is uneconomical to expect bridges to resist large earthquakes elastically (AASHTO 2007). The structural components of the bridge are then designed based on the scaled load, which varies for different materials and importance categories.

Substructure	Importance Category		
	Critical	Essential	Other
Wall-type piers—larger dimension	1.5	1.5	2.0
Reinforced concrete pile bents			
• Vertical piles only	1.5	2.0	3.0
• With batter piles	1.5	1.5	2.0
Single columns	1.5	2.0	3.0
Steel or composite steel and concrete pile bents			
• Vertical pile only	1.5	3.5	5.0
• With batter piles	1.5	2.0	3.0
Multiple column bents	1.5	3.5	5.0

Connection	All Importance Categories
Superstructure to abutment	0.8
Expansion joints within a span of the superstructure	0.8
Columns, piers, or pile bents to cap beam or superstructure	1.0
Columns or piers to foundations	1.0

Figure 2.4 Response Modification Factors in AASHTO LRFD Bridge Design Specifications (2007) (Table 3.10.7.1-1 & 2)

The AASHTO Guide Specifications were developed under the guidance of the AASHTO T-3 Committee as part of a National Cooperative Highway Research Program (NCHRP) task. The method of identifying seismic hazard utilizes identical USGS ground motion hazard maps and life safety performance criteria as the existing specifications. The Guide Specifications also partitions the structure into Seismic Design Categories (SDC) on the same basis as the AASHTO LRFD Bridge Specifications and utilize the response spectrum method for calculating the elastic seismic demand. The Guide Specifications however, employ ductility-based design after the realization that this method of design is significantly less sensitive to sharp increases in the uncertain and variable seismic loading (Elnashai & Sarno, 2008). Ductility-based design evaluates the performance of a structural system based on the capacity of the system to provide ductility through inelastic deformation. The first steps of the specifications are similar to the existing specification; analysis requirements are determined through the use of hazard maps, a design response spectrum and an SDC classification. For Colorado, which falls into SDC A, no

displacement or capacity check is required. The extent of the analysis includes determination of basic design forces, a check against minimum criteria for unseating at supports, along with basic column detailing and foundation design. For SDC B, C and D, the design guidelines incorporate more rigorous analysis and design. SDC B requires displacement capacity check along with suggestions for force capacity checks. SDC C and D involve the engineer's choice of a design strategy referred to as the Earthquake Resisting System (ERS) and development of earthquake resisting elements (ERE). The ERS is designed to provide additional ductility and energy dissipation to the structure, typically in either the substructure or superstructure. This is provided through detailing of plastic hinge regions using specified procedures in the code. In addition, the code supplies design requirements for capacity protection of the elements around the ERS that are designed not to experience damage. The capacity protection method is employed where the individual component resistances should have the ability to resist loads generated when adjacent components reach their overstrength capacity (AASHTO, 2009). Final steps in the SDC B, C, and D involve assessments for ground liquefaction.

2.4 Typical Reinforced Concrete Bridge Types in Colorado

There were approximately 3,447 bridges built in Colorado leading up to the start of 2011, including bridges that are of various span length, structural configurations and material (Colorado Department of Transportation, 2011). Of these, a predominant number are straight, short, simple span reinforced concrete bridges, which tend to exhibit a well-documented dynamic response in comparison to complex bridges. The vulnerability of bridges incorporating both curvature and skew to seismic ground motion excitation are of interest, as these bridges make up a portion of Colorado's bridge inventory.

Skewed highway bridges incorporate a slant in the layout of the bridge superstructure such that it facilitates easy access or egress from complex intersections and dense urban areas. Although the offset angle of the superstructure may present advantages to the transportation layout, the dynamic response of this type of bridge has in the past led to failures, particularly due to unseating, under seismic loading. Examples of this kind of failure of skewed reinforced concrete bridges have been observed after the earthquakes in Northridge (1981), Costa Rica (1991), and more recently in Chile (2010).

An example of a typical skewed bridge failure is the collapse of the Rio Bananito Bridge (Fig. 2.5) following the magnitude 7.6 M_w, Costa Rica Earthquake that occurred in 1991 (Moehle & Eberhard, 2000). The two-span bridge was skewed at 30 degrees at the abutments and piers, and suffered unseating of both spans at the central pier. This is a similar failure mode to that of the Gavin Canyon Undercrossing, which suffered failure during the magnitude 6.6 M_w 1994 Northridge earthquake due to unseating of skewed hinges and collapse of adjacent spans.

Figure 2.5 (Cole, 1991). Costa Rica Earthquake, Rio Bananito Bridge Failure.

There are several studies providing insight on the seismic vulnerabilities of skewed bridges. Presented in a case study by Wakefield (1991), the dynamic response of short stiff skewed bridges is predominantly characterized by in-plane-body-motion including translation and rotation at the abutments. Described in an early study by Maragakis (1984), accompanied by excessive horizontal in-plane deflection are usually bending failures at the tops of the columns, observed particularly in the Northbound Truck Route Undercrossing. Bignell et al. (2005) conducted push-over analysis on typical Illinois bridges and the findings were consistent with that of Margarakis.. Findings from the study by Bignell concluded that the ultimate capacity of the bridge was drastically reduced due to skew angles by nearly two thirds in the longitudinal direction. The effects of large transverse displacements stemming from interaction between the deck and abutment were observed and it was also noted that controlling failure mechanisms not observed in regular bridges occurred.

In a study by Saadeghvaziri and Yazdani-Motlagh (2000), the vulnerability of multispan simply supported bridges with focus on soil structure interaction, was assessed using nonlinear 2D dynamic time-history analysis. It was found that the impact caused by the loading can impose large shear stresses on the bearings of skewed bridges.Previous studies have concluded that decks with skew angles below 30 degrees tend to not display the same complex motion exhibited with larger skew angles and therefore, can be analyzed as straight bridges (S. Maleki 2001; Saiidi & Orie 1992). The same conception appears in legislation of the AASHTO LRFD Bridge Specifications and matches the findings of several other authors.

Curved bridges are susceptible to a similar asymmetrical failure as skewed bridges. The effect of curvature on the seismic response of highway bridges has been examined extensively in many studies, however the work has been predominantly concentrated on steel bridges

(Abdel-Salam and Heins 1989; Burdette et al. 2008; Galindo et al. 2008; Galindo et al. 2009; Linzell and Nadakuditi 2011; Mwafy and Elnashai 2007; Seo and Linzell 2012). An example of where the curved geometry may have contributed to failure was the collapse of the South Connector Overcrossing (Fig. 2.6) during the 1971 San Fernando earthquake of magnitude 6.6 M_w.

Figure 2.6 (Earthquake Engineering Research Institute (EERI), 1996) South Connector Overcrossing Failure

The South Connector Overcrossing (SCO) suffered collapse of two of its deck segments in addition to the column supporting it. The collapse was attributed to unseating of the superstructure in the longitudinal direction at a hinge joint. This caused an acute loading on the column from the cantilevered section and ultimately led to a progressive collapse of the connected column and adjacent span (Williams and Godden 1979). Williams and Godden's work showed that in particular, continuous deck design was crucial in providing transverse stiffness to the superstructure. In non-continuous systems expansion joints became focus points for high stress concentrations and potentially large displacements, which may have led to unseating in some cases.

More recently, Galindo et al. (2009) investigated the effect of four different radii of curvature on the seismic performance of curved steel I-girder bridges and the results showed that the degree of curvature has large effect on bridge response. For example, it was found that shorter radii increases the vulnerability to joint residual damage and pounding effects, attributed to out-of-phase vibrations of spans. Unseating was linked to large rotations in the superstructure at the outside edge of the deck, causing the deck to rotate off support bearings. This matches the findings by Linzell and Nadajuditi (2011), who attributed curvature as the primary parameter affecting seismic load levels at bearings and critical cross frame members. In addition to uplift, large reaction forces were also observed at the ends of interior girders (Galindo et al. 2009). Mwafy and Elnashai (2007) conducted research on the effects of several modeling assumptions on the prediction of demand/capacity ratios of steel bridges, such as bearing friction, design conditions and earthquake intensity. It was found that the modeling assumptions are important to the bridge performance, and that using simplified conservative design decisions may lead to a non-conservative representation of the bridge in some cases (Mwafy and Elnashai 2007).

Numerical studies that assess the seismic performance of both skewed and curved bridge geometries were not found in the literature review conducted. In the studies summarized above, independent analyses show that there are apparent vulnerabilities common to skewed and curved bridges. For example, both bridge configurations appear to be susceptible to deck unseating, tangential joint damage, pounding effects as well as large in-plane displacements and rotations of the superstructure. The responses of the bridge types also appear to be heavily dependent on the levels of skew, curvature, abutment support configuration, and soil structure interaction.

2.5 Vertical Ground Motion

The vertical component of earthquake ground motion is characterized by compressive P-waves of shorter wavelength, while the horizontal component is characterized by secondary, shear S-waves of longer wavelength. The source spectrum of the vertical component has a lower corner frequency compared to the P-wave spectrum, thus attenuation as waves travel away from the source is more prevalent in the vertical, compared to horizontal, direction. The energy content of vertical ground motion also tends to be less than what is observed in horizontal ground motion over a larger frequency range. In contrast to horizontal ground motion, where the energy is distributed through longer periods, the energy in the vertical component tends to be concentrated in a condensed band with short periods (Collier & Elnashai 2001).

The first major investigation into the effect of vertical accelerations on the elastic response of reinforced concrete highway bridges was conducted by Saadeghvariri and Foutch (1991). Three-dimensional finite element (FE) models were constructed of eight 2-span bridges with single and dual bents. Fluctuations in shear capacity resulting from a varying axial force, in addition to reduced energy dissipation capacity in the bents, were attributed to vertical accelerations. Broderick and Elnashai (1995) assessed the failure of a freeway ramp during the 1994 Northridge earthquake using FE models and concluded that static and dynamic analyses utilizing horizontal components only, would not be sufficiently accurate to predict the complete structural behavior and all subsequent failure modes. Collier and Elnashai (2001) concluded that the vertical component of ground motion is significant in near-fault regions, and should be incorporated into design and analysis for site locations less than 25 km from an earthquake source.

The existing design specifications provide little guidance in terms of an analytical approach to consider vertical ground motion. There is no methodological information available in the AASHTO codes (2007). In the Caltrans Seismic Design Criteria (SDC 2006) an equivalent static load method is employed as an added fraction of the dead load, which is only considered for structures with design peak ground accelerations (PGA) larger than 0.6 g. Vertical P-waves attenuate quickly, as shown in the data presented by Ambraseys and Simpson (ESEE 2001), and for far field site locations the approach employed by structural codes can be conservative. When incorporating vertical ground motion into a seismic analysis, a common approach originally suggested by Newmark et al. (1973), proposes scaling based on a single spectral shape. The spectrum is developed for the horizontal ground motion, and utilizes a 2/3 vertical-to-horizontal (V/H) acceleration ratio to account for vertical effects. For near field site locations however, both approaches can result in underestimation of the effects. This is apparent from the discussion of the frequency content, but it has also been well demonstrated in a large number of studies including, but not limited to Abrahamson and Litehiser (1989), Bozorgonia and Campbell (2004), Elgamal and He (2008), Kim et al. (2011). Furthermore, Collier and Elnashai (2001) conducted an extensive study where the V/H ratio was confirmed to exceed ratios larger than 1 for fault distances smaller than a 5 km radius from the source of the earthquake, and larger than 2/3 at a 25 km radius depending on the earthquake magnitude.

In addition to seismic contribution of the vertical ground motion component, the arrival time of the horizontal and vertical components of ground motion as well as their relative difference is also considered to be important to the structural response. Silva (1997) demonstrated through patterned analysis of vertical time histories that short-period vertical ground motion was likely to arrive before subsequent S-waves, while longer-period vertical ground motion arrived at

equivalent times. Collier and Elnashai (2001) investigated the difference in arrival time through investigation of two seismic events. The analysis concluded that the time interval at which the waves were separated increased proportional to site distance, with equivalent arrival times observed for site distances less than 5 km from the fault. Kim et al. (2011) found in their investigation of the effect of arrival time on the performance of RC bridge pier-columns, that the time interval had a relatively minimal effect on the axial and shear demand, but had a rather significant effect on the shear capacity.

2.6 Analysis Methods for Estimating Seismic Demand

There are several available methods for estimating the demand imposed by earthquakes on bridge structures. The conventional analysis methods adopted in research and structural code are discussed in the following section. The methods covered include: nonlinear pushover analysis for estimation of ultimate capacity; modal analysis, employed for assessment of modal vibration; response spectrum method, which evaluates the response based on peak force capacity at the fundamental mode of vibration; and time history analysis, for real time simulation of earthquake loading.

Nonlinear pushover analysis is a common analytical technique employed in research and design for evaluating the structural behavior of bridges in the inelastic range as well as identify locations of critical weakness (Bignell et al. 2005; Krawinkler & Seneviratna 1998; Washington Department of Transportation 2011). Conventional pushover analysis consists of applying a monotonically increasing lateral forcing function at a structural center point until an upper limit state or failure is attained. The lateral load distribution applied may be proportional to the fundamental mode shape, provided that 75% of the structural mass participates in the particular mode (FEMA 356 2000). The results of the pushover analysis are typically expressed as base

shear at the pier versus the lateral displacement or rotation at the bent. A number of target displacements are identified and the resulting strength demands are compared with the available structural capacity.

Modal analysis is used to assess the mass participation of the structure in different modes of vibration. It serves as a basis for all other analyses by determining the predominant response of the structure and the period at which it will vibrate. Typically, a multi-degree-of-freedom (MDOF) structural model is excited using a transient signal and decomposed analytically into a series of single degree of freedom systems. The response of the system is then calculated in the time domain and algebraically combined to yield the global response of the MDOF system. This method is considered a time-domain solution and is applicable only to linear-elastic systems as it utilizes superposition.

Response spectrum method is utilized to assess the peak response of a structure, and is commonly used in structural code such as the AASHTO LRFD Bridge, and Guide Specifications for moderate seismic zones (AASHTO, 2007). The analytical method is governed by the following equations of dynamic equilibrium as a response to ground motion:

$$Mx\ddot{(t)} + Cx\ddot{(t)} + Kx(t) = m_x\ddot{x}_{gx}(t) + m_y\ddot{x}_{gy}(t) + m_z\ddot{x}_{gz}(t)$$

where K represents the stiffness matrix, M represents the diagonal mass matrix and C represents the proportional damping matrix; The variables of x(t) represent the motion with respect to the ground, $\ddot{x}_{gx,y,z}$ represents the components of uniform ground acceleration, and lastly $m_{x,y,z}$ represents the unit acceleration loads (CSI 2011). Response spectrum analysis evaluates the model at the maximum response to the dynamic equilibrium equation at the fundamental period of vibration. The input is a response spectrum curve of spectral acceleration versus structural period. This is developed using the simplified guidelines exhibited in structural code. The

computed dynamic response of the bridge structure represents a statistical calculation of the maximum magnitude for that measure. Response-spectrum analysis is generally based upon superposition with modes computed using Ritz-vector analysis.

Non-linear time history analysis (NLTHA) is the most precise form of analysis for representing seismic loads. NLTHA is recognized as the most accurate and rigorous analysis method and is widely utilized in both complex and commercial finite element software (Burdetteet al. 2008; Mwafy & Elnashai, 2007). NLTHA is a step function analysis and evaluates the dynamic response of the bridge structure due to a specific earthquake loading. The equations of motion defining this type of analysis are as follows:

$$M\ddot{x}(t) + C\ddot{x}(t) + Kx(t) = F(t)$$

Where K, M, and C, represent the stiffness matrix, the mass matrix, and the damping matrix, respectively and x(t) and $F(t)$ represent the displacement increment at a specified time increment and the forcing function, respectively. The forcing function is typically represented by an earthquake record, scaled to the level of seismic hazard of the bridge, discussed in the following section. Direction integration utilizing the Hilber-Hughes-Taylor method is selected as the method of calculating the equations of motion for each time step (Hilber et al. 1979). Direct integration offers the advantages of displaying full damping properties of coupled modes, and more efficient integration of wave and impact propagation of higher modes. The Hilber-Hughes-Taylor method is optimal for non-linear analysis where the reduction in stiffness may lead to excitation of higher modes in later time steps; however it is extremely sensitive to the time step (CSI 2011).

2.7 Ground Motion Scaling

Nonlinear time-history analysis subjects the numerical model to an array of ground motion records. Prior to this step however, the records require scaling to match the seismic exposure of the area. There are several methods that can be used to scale ground motion records. The following methods discussed include: the code based approach of scaling at single spectral periods; scaling based on max incremental velocity and spectral intensity; modal-pushover based approach and lastly a description of methods that have been shown to produce inaccuracies. The approach taken in this study utilizes the code-based approach of scaling at single spectral periods for the study based in the Mountain West region in Chapter 3; while a more varied approach is taken using Arias Intensity when addressing the vertical ground motion component in Chapter 4.

Following the methodology presented in the AASHTO Guide Specifications, the code-based approach scales the spectral response of the record to a design response spectrum at the fundamental period of the structure. The requirements for the ground motions dictate that a minimum of three compatible time histories should be utilized to represent the design earthquakes. In addition, the earthquake records should be obtained from geological conditions representing similar shear wave velocity characteristics and have similar magnitudes and distances as to reduce the scaling factor. The scaling of spectral accelerations at single spectral periods as presented in the guidelines in the code, has also been widely utilized in research (Kunnath et al. 2006; among others).

In addition to the code-based approach, there are several other appropriate methods for ground motion scaling. Kurama and Farrow (2003) introduced a method of scaling based on the maximum incremental velocity. Baker and Cornell (2006), proposed that if earthquake records are selected with appropriate spectral shape, the structural response reduction and amplifications

are comparable to the variation in earthquake intensity. The most recent developments in ground motion scaling came from Kalkan and Chopra (2010) and Kalkan and Kwong (2010), who developed modal-pushover-based scaling approaches.

Other methods of scaling have been shown to produce inaccuracy and large variances in response. For example, scaling based on the peak ground acceleration (PGA) has been shown to produce large scatter (Vidic et al. 1994, Shome & Cornell 1998). Kuruma and Farrow (2003), summarized that scalar intensity measures such as effective peak acceleration, and effective peak velocity can be inaccurate and insufficient for analysis. A comprehensive summary and evaluation of the scaling methods listed above as well as other methods can be found in a National Science Foundation (NSF) report authored by Donnell et al. (2011).

The spectrum intensity method proposed by Housner (1952), similarly bases its foundation on that the elastic response spectra, calculated from the velocity record, can be integrated to estimate seismic energy (Housner 1952). The velocity spectrum provides a source for induced energy on the structure and is subsequently linked to the structural response and induced damage. The intensity of an earthquake is defined as the area under the elastic velocity spectrum between the periods of 0.1 and 2.5, which represents typical periods of vibration of bridge structures.

2.8 Bridge Modeling with Advance Finite Element Software

After the ground motions are selected and the methods of analysis are established, a model that accurately represents the response of the bridge structure is needed. There are several model types that are applicable to providing a representation of the structural characteristics of bridges, although they have varying degrees of accuracy and time efficiency. These include single degree of freedom (SDOF) systems, MDOF models, and detailed finite element (FE) models. SDOF

models have the advantage of necessitating low computational demand and yield a fair representation of the global behavior. SDOF models are however limited primarily to standard bridge structures and do not account for tridimensional effects and local behavior (Elnashai & Sarno, 2008). Stick models account for multiple degrees of freedom, are applicable to all types of structures, and accommodate tridimensional effects. But similar to SDOF models, stick models only account for the global response. In a recent publication by Abdel-Mohti and Pekan (2008) on the comparison between detailed finite element models and beam stick models for skewed bridges in SAP 2000, it was concluded that for bridge decks with skew angles larger than 30 degrees, detailed finite element models should be employed in order to correctly represent higher mode effects. Detailed finite element models are the most complex and widely utilized model type and are the preferred modeling method to represent both the global and local structural behavior under dynamic loading.

Finite element models using SAP2000 have been extensively developed by many researchers in seismic engineering. Mwafy and Elnashai (2007) investigated the seismic integrity of multi-span curved bridges using SAP2000. Itani and Pekcan (2011) investigated the seismic performance of steel plate girder bridges with integral-abutments using SAP2000. Kappos et al. (2005) utilized the analysis program to show that modal-pushover analysis can be effectively employed for seismic assessment of bridges. SAP2000 is also currently implemented in several design offices for seismic analysis. Washington DOT utilizes SAP2000 and AASHTO Guide specifications as the basis for evaluation of bridge structures and have developed guidelines and design examples (Washington Department of Transportation 2011). It is also used for seismic analysis by State Departments of Transportations in Indiana, Nevada, California and New Hampshire.

2.9 References

AASHTO. (2007). *AASHTO LRFD Bridge Design Specifications* (4th ed.). Washington, DC: AASHTO.

AASHTO. (2009). *AASHTO Guide Specifications for LRFD Seismic Bridge Design* (1st ed.). Washington, DC: AASHTO.

Abdel-Mohti, A., & Pekcan, G. (2008). Seismic Response of Skewed RC Box-Girder Bridges. *Earthquake Engineering and Engineering Vibration*, *7*(4), 415–426. doi:10.1007/s11803-008-1007-4

Abdel-Salam, M., & Heins, C. (1988). Seismic Response of Curved Steel Box Girder Bridges. *Journal of Structural Engineering*, *114*(12), 2790–2800. Retrieved from http://ascelibrary.org/doi/abs/10.1061/(ASCE)0733-9445(1988)114%3A12(2790)

Abrahamson, N. A., & Litehiser, J. J. (1989). Attenuation of Vertical Peak Acceleration. *Seismological Society of America*.

American Society of Civil Engineers. (n.d.). *FEMA 356-Prestandard and Commentary for the Seismic Rehabilitation of Buildings*. *Washington DC: Federal Emergency Management …*. Washington, DC.

Baker, J. W., & Allin Cornell, C. (2006). Spectral shape, epsilon and record selection. *Earthquake Engineering & Structural Dynamics*, *35*(9), 1077–1095. doi:10.1002/eqe.571

Bignell, J. L., LaFave, J. M., & Hawkins, N. M. (2005). Seismic vulnerability assessment of wall pier supported highway bridges using nonlinear pushover analyses. *Engineering Structures*, *27*(14), 2044–2063. doi:10.1016/j.engstruct.2005.06.015

Bozorgnia, Y., & Campbell, K. W. (2004). the Vertical-To-Horizontal Response Spectral Ratio and Tentative Procedures for Developing Simplified V/H and Vertical Design Spectra. *Journal of Earthquake Engineering*, *8*(2), 175–207. doi:10.1080/13632460409350486

Broderick, B. M., & Elnashai, a. S. (1995). Analysis of the failure of interstate 10 freeway ramp during the Northridge earthquake of 17 January 1994. *Earthquake Engineering & Structural Dynamics*, *24*(2), 189–208. doi:10.1002/eqe.4290240205

Burdette, N. J., Elnashai, A. S., Lupoi, A., & Sextos, A. G. (2008). Effect of Asynchronous Earthquake Motion on Complex Bridges. I: Methodology and Input Motion. *Journal of Bridge …*, (April), 158–165.

California Department of Transportation. (2006). Caltrans Seismic Design Criteria, (1.6), 161. Retrieved from http://www.dot.ca.gov/hq/esc/earthquake_engineering/SDC/

Charlie, W. A., Battalora, R. J., Siller, T. J., & Doehring, D. O. (2002). Magnitude Recurrence Relations for Colorado Earthquakes. *Earthquake Spectra*, *18*(2), 233. doi:10.1193/1.1490546

Charlie, W., Battalora, R., Siller, T., & Doehring, D. (2006). Colorado Earthquakes and Active Faults, 20–34.

Collier, C. J., & Elnashai, a. S. (2001). a Procedure for Combining Vertical and Horizontal Seismic Action Effects. *Journal of Earthquake Engineering*, *5*(4), 521–539. doi:10.1080/13632460109350404

Colorado Department of Transportation. (2011). *Transportation Facts*. Denver.

Computers and Structures Inc. (2011). *CSI Analysis Reference Manual*. Berkeley, California, USA.

Cooper, J., Sharpe, R. L., Fox, G. F., Gates, J. H., Goins, V. M., Hourigan, E. V, Mayes, R. L., et al. (1981). *ATC- 6 Seismic Design Guidelines for Highway Bridges*. Berkeley, California, USA.

Donnell, A. P. O., Beltsar, O. A., Kurama, Y. C., & Taflanidis, A. (2011). Evaluation of Ground Motion Scaling Methods for Nonlinear Analysis of Structural Systems Erol Kalkan Unites States Geological Survey. *Proceedings of 2011 NSF Engineering Research and Innovation Confernence*. Atlanta, Georgia.

Douglas, J. (2001). A comprehensive worldwide summary of strong-motion attenuation relationships for peak ground acceleration and spectral ordinates (1969 to 2000). *Engineering Seismology and Earthquake Engineering*, (01-1).

Elgamal, A., & He, L. (2008). Vertical Earthquake Ground Motion Records: An Overview. *Journal of Earthquake Engineering*, (April 2013), 37–41.

Elnashai, A. S., & Luigi Di Sarno. (2008). *Fundamentals of Earthquake Engineering* (1st ed., p. 347). John Wiley & Sons, Ltd.

Foutch, D. A., & Saadeghvariri, M. A. (1991). Dynamic Behaviour of R/C Highway Bridges Under the Combined Effect of Vertical and Horizontal Earthquake Motions. *Earthquake Engineering Structural Dynamics*, *20*(6), 535–549. doi:10.1002/eqe.4290200604

Galindo, C., Hayashikawa, T., & Julian, D. (2008). Seismic Damage due to Curvature Effect on Curved Highway Viaducts. *jetty.ecn.purdue.edu*.

Galindo, C. M., Hayashikawa, T., & Belda, J. G. (2009). Damage Evaluation of Curved Steel Bridges Upgraded with Isolation Bearings and Unseating Prevention Cable Restrainers, 53–61.

He, X. H., Sheng, X. W., Scanlon, a., Linzell, D. G., & Yu, X. D. (2012). Skewed concrete box girder bridge static and dynamic testing and analysis. *Engineering Structures*, *39*, 38–49. doi:10.1016/j.engstruct.2012.01.016

Housner, G. W. (1952). Spectrum Intensities of strong-motion earthquakes. *Proceedings of the 1st World Conference on Earthquake Engineering,*, *1*.

Kalkan, B. E., & Kwong, N. S. (2010). Documentation for Assessment of Modal Pushover-Documentation for Assessment of Modal Pushover-Based Scaling Procedure for Nonlinear Response History Analysis of "Ordinary Standard" Bridges.

Kalkan, E., & Chopra. (2010). Practical guidelines to select and scale earthquake records for nonlinear response history analysis of structures. *US Geological Survey Open-File Report*.

Kappos, A. J., Paraskeva, T. S., & Sextos, A. G. (2005). Modal pushover analysis as a means for the seismic assessment of bridge structures. *4th European Workshop on the Seismic Behaviour of Irregular and Complex Structures*. Thessaloniki, Greece.

Kawashima, K., Unjoh, S., & Hoshikuma, J. (2010). Damage of transportation facility due to 2010 Chile Earthquake.

Kim, S. J., Holub, C. J., Elnashai, A. S., & Asce, F. (2011). Analytical Assessment of the Effect of Vertical Earthquake Motion on RC Bridge Piers, (February), 252–260.

Kirkham, R. (1986). An interpretation of the November 7, 1882 Colorado earthquake. *Colorado Geological Survey*, (Open File Report 86-8). Retrieved from http://onlinelibrary.wiley.com/doi/10.1002/cbdv.200490137/abstract

Kirkham, R. M., & Rogers, W. P. (1985). Colorado Earthquake Data and Interpretations 1857 to 1985. *Colorado Geological Survey*, *46*, 94.

Krawinkler, H., & Seneviratna, G. D. P. K. (1998). Pros and cons of a pushover analysis of seismic performance evaluation. *Engineering Structures*, *20*(4-6), 452–464. doi:10.1016/S0141-0296(97)00092-8

Kunnath, S. K., Larson, L., & Miranda, E. (2006). Modelling considerations in probabilistic performance-based seismic evaluation: case study of the I-880 viaduct. *Earthquake Engineering & Structural Dynamics*, *35*(1), 57–75. doi:10.1002/eqe.531

Kurama, Y. C., & Farrow, K. T. (2003). Ground motion scaling methods for different site conditions and structure characteristics. *Earthquake Engineering & Structural Dynamics*, *32*(15), 2425–2450. doi:10.1002/eqe.335

Linzell, D., & Nadakuditi, V. (2011). Parameters influencing seismic response of horizontally curved, steel, I-girder bridges. *Steel and Composite Structures*, *11*(1), 21–38.

Maleki, S. (2001). Free Vibration of Skewed Bridges. *Journal of Vibration and Control*, *7*(7), 935–952. doi:10.1177/107754630100700701

Maragakis, E. (1984). *A model for the rigid body motions of skew bridges*. Pasadena, California. Retrieved from http://resolver.caltech.edu/caltechEERL:1984.EERL-85-02

Moehle, J., & Eberhard, M. (2000). *Earthquake damage to bridges*. (W.-F. Chen & L. Duan, Eds.)*Bridge Engineering Handbook*. CRC Press, 2000.

Mwafy, A. M., & Elnashai, A. S. (2007). Assessment of seismic integrity of multi-span curved bridges in mid-America, (April).

Newmark, N. M., Asce, H. M., & Engrg, C. (2010). Seismic Design Spectra for Nuclear Power Plants. *Atomic Energy*, *99*(PO2), 1973.

Saadeghvaziri, M. A., Yazdani-Motlagh, A. R., & Rashidi, S. (2000). Effects of soil ± structure interaction on longitudinal seismic response of MSSS bridges. *Soil Dynamics and Earthquake Engineering*, *20*, 231–242.

Saiidi, M., & Orie, D. (1992). Earthquake design forces in regular highway bridges. *Computers and Structures*, *44*(5), 1047–1054.

Seo, J., & Linzell, D. G. (2012). Nonlinear Seismic Response and Parametric Examination of Horizontally Curved Steel Bridges Using 3-D Computational Models. *Journal of Bridge Engineering*. doi:10.1061/(ASCE)BE.1943-5592.0000345

Sheehan, A. F., Godchaux, J. D., & Hughes, N. (2003). Colorado Front Range Seismicity and Seismic Hazard. *Colorado Geological Survey Special Publication 55*, (15), 1–21.

Silva, W. (1997). Characteristics of vertical strong ground motions for applications to engineering design. *FHWA/NCEER Workshop on the Nat'l Representation of Seismic Ground Motion for New and Existing Highway Facilities*, (Technical Report NCEER-97-0010).

Spence, W. (1999). Colorado's Largest Historical Earthquake. *USGS Fact Sheet 098-99*, (098-99).

Spence, W., Langer, C. J., & George, L. C. (1996). Rare , Large Earthquakes at the Laramide Deformation Front Colorado (1882) and Wyoming (1984), *86*(6), 1804–1819.

Stover, C. W., & Coffman, J. L. (1993). Seismicity of the United States, 1968-1989 (Revised). *U.S. Geological Survey Professional Paper 1527*, 418.

Wakefield, R., & Nazmy, A. (1991). Analysis of seismic failure in skew RC bridge. *Journal of Structural Engineering*, *117*(3), 972–986.

Washington Department of Transportation. (2011). *WSDOT Bridge Design Manual*.

Widmann, B. L., Kirkham, R. M., & Rogers, W. P. (1998). *Preliminary Quaternary Fault and Fold Map and Database of Colorado*. *Colorado Geological Survey* (Vol. Open-File). Denver, Colorado.

Chapter 3: Seismic Performance of Skewed and Curved Reinforced Concrete Bridges in Mountainous States

3.1 Introduction

Horizontally curved and skewed bridges are becoming an increasingly prominent component of modern highway transportation systems due to their ability to accommodate geometric restrictions imposed by existing highway components. In contrast to these advantages, skewed and curved bridges experience a less predictable dynamic behavior and more complex demands when subjected to a seismic event. The abutment type is also an important component when examining the seismic performance of highway bridges. Integral abutments are widely utilized because they offer advantages to construction cost, long term maintenance, and structural performance by reducing impact loads through removal of expansion joints. In the present study, parametric analysis is conducted on the seismic performance of skewed and curved RC three-span bridges in the Mountain West region. The bridges examined follow typical design for the region, including the adoption of continuous deck design and integral abutments. The parametric analysis investigates a suite of bridges with various configurations of skew and/or curvature that utilize identical structural components. The research is targeted at gaining a better understanding of the global behavior of various bridge configurations during a low to moderate seismic event. Furthermore, critical locations for failure will be identified such that seismic design of these structures, independent of geographic location, may be more informed and safe. To begin with, a literature review of related studies is made. Secondly, a nonlinear FEM numerical model of the baseline bridge with a common curvature and skew design is developed and analyzed. Finally, a comprehensive parametric study is conducted to evaluate the impacts of different variables

including loading direction, level of skew and curvature, and support condition, on seismic performance.

3.2 **Background and Motivation**

Seismic performance of skewed bridges

Although skewed bridges offer benefits to transportation design, the offset angle of the superstructure has in the past led to seismic-induced failure, particularly due to excessive deflections of the superstructure. For example, moderate earthquakes in Costa Rica (1991), Northridge (1994) and more recently in Chile (2010), have induced failures in skewed RC bridges. Wakefield (1991) and Maragakis (1984) studied the dynamic behavior of skewed bridges and observed failure of the Foothill Boulevard Undercrossing. Failure was characterized by unseating and column damage, attributed to rigid-body motion in the superstructure. In a study by Saadeghvaziri and Yazdani-Motlagh (Saadeghvaziri et al. 2000), it was found that seismic-induced impact between spans of skewed bridges can impose large shear stresses on bearings, and that soil-structure interaction can have significant effect on bridge behavior. Pushover analysis conducted by Bignell et al. (2005) showed that incorporating skew on bridges can significantly reduce the comparative ultimate capacity during a seismic event by up to 2/3 in the longitudinal direction. Various studies indicated that bridges with skew angles below 30 degrees tend away from the higher mode effects, and can often be analyzed as straight or represented without using complex finite element (FE) models (Mohti and Pekcan 2008; Maleki 2002). Recent research has also concluded that the dynamic behavior of skewed bridges is a function of not only the skew angle but also the plan geometry (Dimitrakopoulos 2011).

Seismic performance of curved bridges

Curved bridges are susceptible to a similar asymmetrical failure as skewed bridges. The effect of curvature on the seismic response of highway bridges has been examined extensively in many studies, however the work has been predominantly concentrated on steel bridges (Abdel-Salam and Heins 1989; Burdette et al. 2008; Galindo et al. 2008; Galindo et al. 2009; Linzell and Nadakuditi 2011; Mwafy and Elnashai 2007; Seo and Linzell 2012). Failure of the South Connecting Overpass during the 1971 San Fernando earthquake and analysis conducted by Williams and Godden (1979) identified early vulnerabilities in curved bridges. In particular, continuous deck design was shown to be crucial in providing transverse stiffness to the superstructure. In non-continuous systems expansion joints became focus points for high stress concentrations and potentially large displacements, which may have led to unseating in some cases. More recently, Galindo et al. (2009) investigated the effect of four different radii of curvature on the seismic performance of curved steel I-girder bridges and the results showed that the degree of curvature has large effect on bridge response. For example, it was found that shorter radii increases the vulnerability to joint residual damage and pounding effects, attributed to out-of-phase vibrations of spans. Unseating was linked to large rotations in the superstructure at the outside edge of the deck, causing the deck to rotate off support bearings. This matches the findings by Linzell and Nadajuditi (2011), who attributed curvature as the primary parameter affecting seismic load levels at bearings and critical cross frame members. In addition to uplift, large reaction forces were also observed at the ends of interior girders (Galindo et al. 2009). Mwafy and Elnashai (2007) conducted research on the effects of several modeling assumptions on the prediction of demand/capacity ratios of steel bridges, such as bearing friction, design conditions and earthquake intensity. It was found that the modeling assumptions are important to

the bridge performance, and that using simplified conservative design decisions may lead to a non-conservative representation of the bridge in some cases (Mwafy and Elnashai 2007).

Seismic performance of curved and skewed bridges

Numerical studies that assess the seismic performance of both skewed and curved bridge geometries were not found in the literature review conducted. In the studies summarized above, independent analyses show that there are apparent vulnerabilities common to skewed and curved bridges. For example, both bridge configurations appear to be susceptible to deck unseating, tangential joint damage, pounding effects as well as large in-plane displacements and rotations of the superstructure. The responses of the bridge types also appear to be heavily dependent on the levels of skew, curvature, abutment support configuration, and soil structure interaction.

3.3 **3-D Finite Element Modeling and Seismic Analysis**

Structural components

The bridges analyzed in this study are of varying geometric configurations but are all constructed with the same structural components. The bridge superstructures (Fig. 3.1a) are composed of a 205 mm in concrete slab deck supported by eight, 1.73 m deep, parallel pre-stressed concrete I-girders (Fig. 3.1c). The girders are reinforced longitudinally at the tops of the cross sections and are braced with stirrups at 45 cm intervals. The junctions between adjacent girders, supported by the pier cap, are embedded in a concrete diaphragm creating an integral, fixed connection. Supporting the concrete diaphragms are rectangular pier caps of 1.53 m depth, each supported by an interior and exterior columns with constant average depths (Fig. 3.1b). Each column contains standard longitudinal reinforcement, and transverse rebar confinement at spacing of 83 cm. The abutments and piers are parallel and skewed at the same angle to the

transverse axis. The integral abutment is cast such that it encases the contiguous I-girders, and is also tied by reinforcement to the adjacent deck.

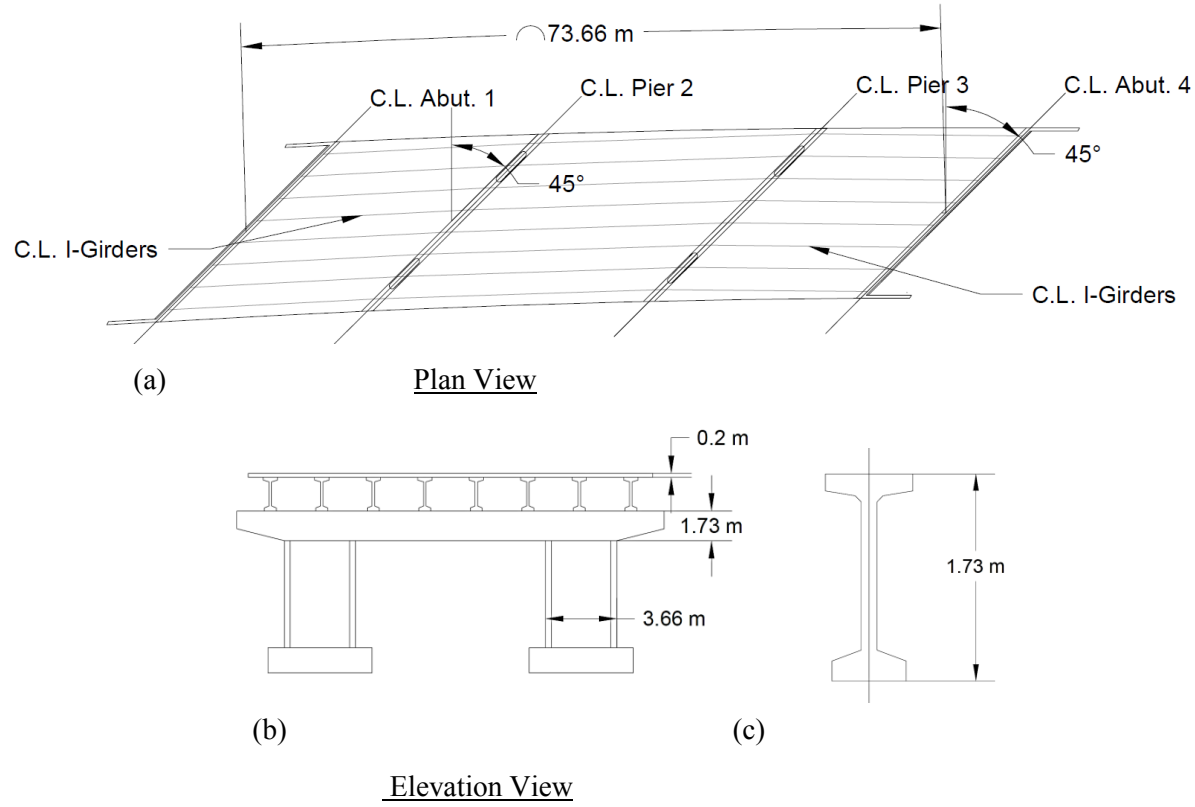

Figure 3.1 (a) Plan View of Bridge – Radius 910 m. Skew 450 **(b)** Pier X-Section and (c) I-Girder X-section

Development of the Finite Element Models

The structural performance of the bridges selected for this study is evaluated using 3-D finite element (FE) models (Fig. 3.2) constructed in SAP2000 (CSI 2011). The method of model construction follows the practices developed by authors in previous studies who have utilized SAP2000, guidelines utilized used for analysis of bridges in high seismic regions, and recommendations made by the software developer (Kappos et al. 2005, Mwafy and Elnashai 2007; Itani and Pekcan 2011; WSDOT 2011; CSI 2011)

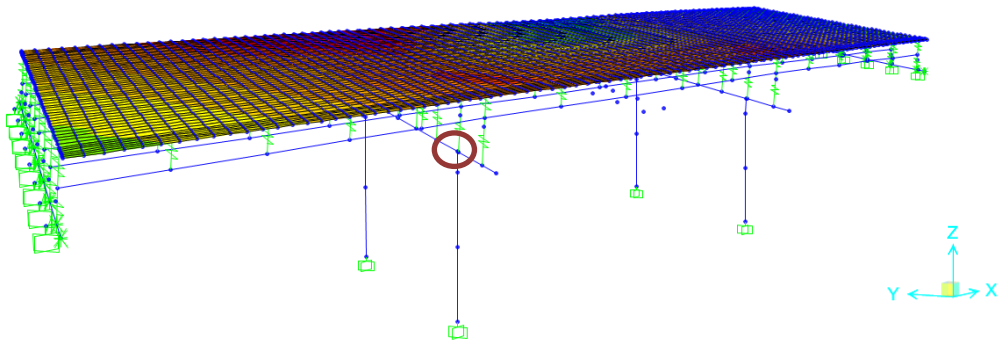

*Location 1 – Circled

Figure 3.2 SAP2000 Finite Element Model of the Bridge

Details of the modeling method are discussed in this section. The bridge deck is modeled using thin shell elements that span intermediate nodes of the girder element and are further meshed into quadrants. Due to minimal contribution to the structural response, reinforcement of the deck is neglected. The girders are modeled using linear beam elements and divided into 5 segments per span in accordance with AASHTO Guide Specifications (5.4.3) (AASHTO 2009). Prestressing components are modeled using lumped tendons at each girder, and the prestressing force (after losses) is applied as end-wise point loads. Beam elements are connected to above shell elements, by the use of fully constrained rigid links. The substructure is modeled using beam elements representing the columns and pier caps. The columns are fixed at the soil foundations in all six rotational and translational directions. The columns are tied directly to the pier cap and adjusted by the use of end length offsets. In order to account for inelastic column behavior, plastic hinges are assigned at a specific distance from the top and bottom of the columns. The hinging mechanism follows the established details by Caltrans, and the locations are developed in accordance with WashDOT procedures (Caltrans 2004; WSDOT 2011).

The integral abutment is modeled using beam elements representative of the abutment cross section. The abutment-girder connection is modeled using a rigid link, characteristic of the

integral fixity between the abutment and girder (CSI 2011). The abutment is considered to have fixity from the surrounding soil and pile foundation in all degrees of freedom except the longitudinal. The backing soil behind the abutment is represented by the use of a multi-linear, longitudinal, compressive spring (Fig. 3.3) following the Caltrans design procedures for backing soil behind an integral abutment (Caltrans 2004).

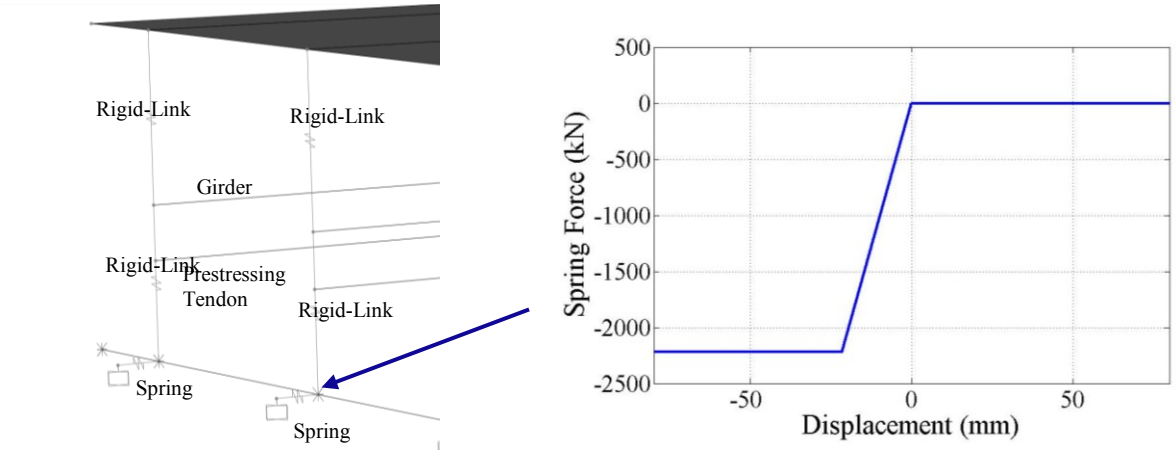

Figure 3.3 Abutment Spring and Force-Displacement Relationship

Ground motion selection and scaling for mountainous states

Seven sets of earthquake records are selected in accordance with AASHTO (2009) Guide Specifications from the Pacific Earthquake Engineering Research (PEER) Center strong motion database (Fig. 4). To simulate typical earthquake motion for states in the Mountain West region, Denver, Colorado is chosen as a site location. A stiff soil profile for Denver is selected, and a design response spectrum is developed using the USGS database and AASHTO (2009) Guide Specifications. Strong motion records are chosen based on a moment magnitude range between Mw 6.5 and 7.0, a stiff soil condition with shear wave velocity range of 300 - 550 m/s, and a 20 - 30 km range for the Joyner-Boore distance of the fault to the site (Rjb). The characteristics of the selected ground motions are listed in Table 3.1. Figure 3.5 shows a representation of the fault normal response spectra for the selected records, and the design response spectrum developed for

the site condition. The scaling factor, is computed for the fault normal and parallel directions, by matching the AASHTO design response spectrum (AASHTO 2009) to the average of the seven earthquake response spectrums at the fundamental period of the bridge structure.

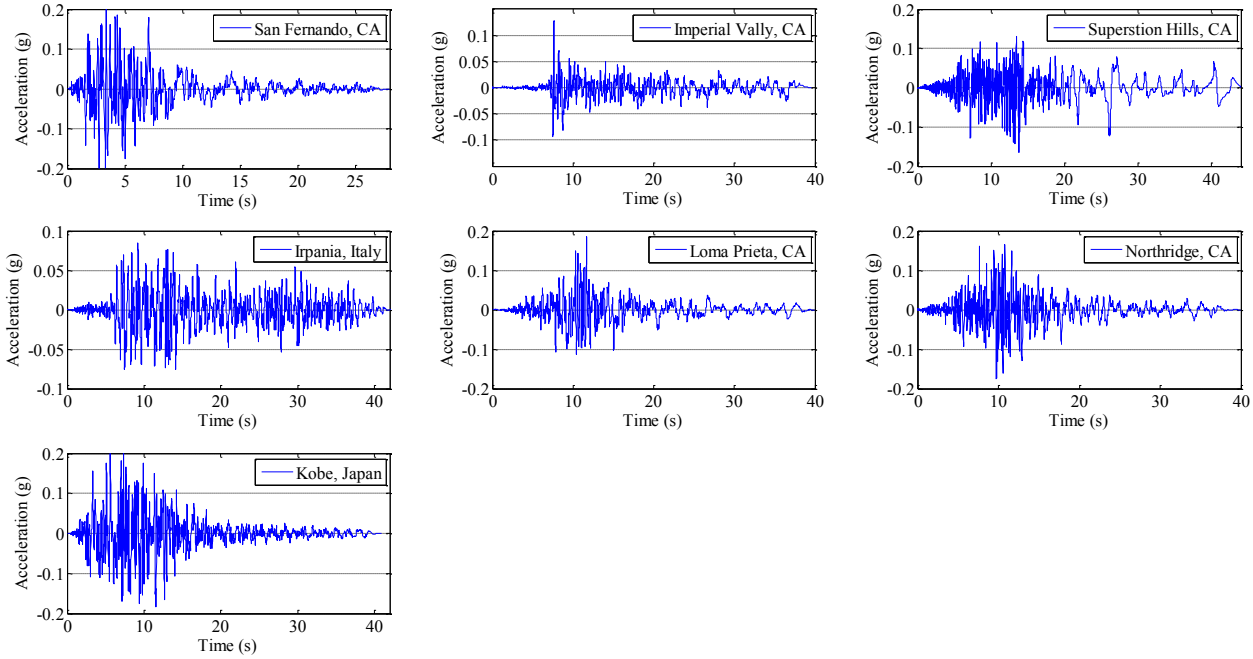

Figure 3.4 Earthquake Time-Histories Used in the Analysis

Table 3.1 Earthquake Characteristics

Record #	Event	Year	Station	Mag. (M_w)	Significant Duration (5-95%, s)	R_{jb} (km)	Vs30 (m/s)
1	San Fernando	1971	LA - Hollywood Stor FF	6.61	11.9	22.9	464.2
2	Imperial Valley	1979	Calipatria Fire Station	6.53	25.1	23.2	301.8
3	Superstition Hills	1987	Wildlife Liquef. Array	6.54	29.1	24.0	304.3
4	Irpinia, Italy	1980	Mercato San. Severino	6.9	28.4	29.8	513.3
5	Loma Prieta	1989	Agnews State Hospital	6.93	18.4	24.3	351.6
6	Northridge	1994	LA - Baldwin Hills	6.69	17.6	23.5	435.7
7	Kobe, Japan	1995	Kakogawa	6.9	17.6	22.5	457.6

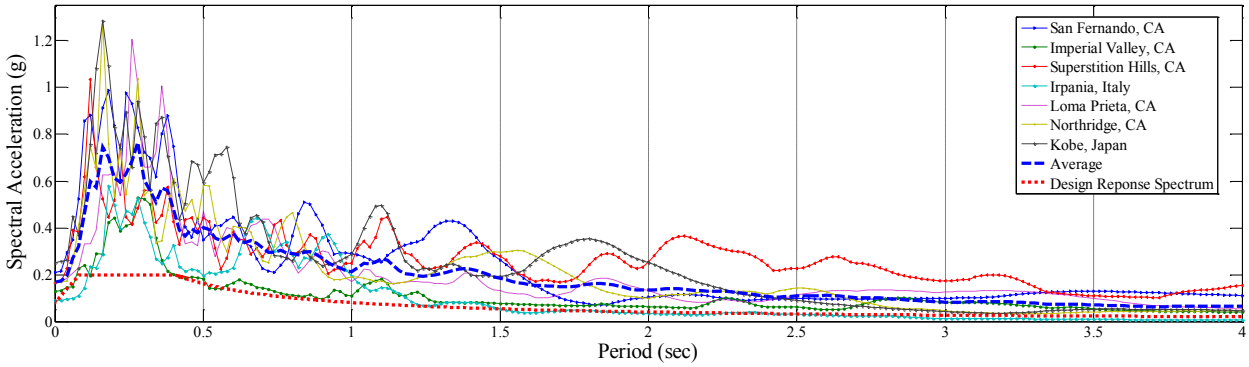

Figure 3.5 Earthquake and AASHTO Design Response Spectrum

Nonlinear time-history analysis procedures

Nonlinear time-history analysis is conducted using the direct integration method. Included in the analyses are material and geometric nonlinearities. Fixed Rayleigh damping coefficients are used that represented 2% damping in the first and second modes. The method of time integration follows the Hilber-Hughes-Taylor method with alpha, beta and gamma values at 0, 0.25, and 0.5, respectively. The integration time step is kept constant at 0.01 sec and a standard iteration convergence tolerance of 0.0001 is used following a sensitivity analysis. Vertical ground motion is typically incorporated into analysis of bridges in high seismic regions and bridges in close proximity to active faults (Button et al. 2002; Caltrans 2004). Given the geographic nature of mountain states and seismic classification, the study considers effects of horizontal ground motions only. Two orthogonal components of the ground motion set are employed simultaneously in each analysis. The fault normal component of the ground motion is employed in the global longitudinal direction, while 40 percent of the fault parallel component is applied in the global transverse direction (Maleki et al. 2006).

3.4 **Configuration of Bridges in Parametric Study and Modal Analysis Results**

The parametric study consists of two parts including: (Part 1) analysis of a baseline model, with variations made to loading direction and abutment support; (Part 2) analysis and comparison of various configurations of skew and curvature. Before the parametric analysis results are discussed in the following section, the skewed and curved bridge configurations are introduced, and the results of a modal analysis are presented.

Part I - Baseline bridge model configuration (Radius: 1730 m; Skew: 30)

Part one of the study examines a baseline bridge model with a single degree of skew and radii of curvature in great detail, and identifies critical areas of interest that will be the focus points later in the parametric study. In addition, it also examines the impact of typical design decisions such as the abutment support condition, and the directional components of the loading (Table 3.2). The baseline bridge model includes a radius of curvature of 1730 m (4500 feet), a skew angle of 30 degrees, and a super elevation of 4 degrees. The geometric specifications meet dimensional requirements utilized by the Colorado Department of Transportation bridge design office and detailing is taken directly from a highway bridge on I-25 in Northern Colorado. A plan view and an elevation view of the baseline bridge configuration is shown in Figure 3.6a and 3.6b, respectively,

Table 3.2 Bridge Components for Baseline Comparison

Scenario	Skew (degrees)	Curvature Radius (m)	Component
1	30	1370	Baseline Model
2	30	1370	Reversed Directional Loading
3	30	1370	Bearing Support

Part II - Geometric configurations of bridges

The second part of the parametric study examines eight RC bridges of varying curvature and skew, constructed from the baseline model for parametric comparison. The bridge configurations were chosen with guidance from the Colorado Department of Transportation and are representative of a large range of typical skewed and curved bridges in Colorado. Each bridge consists of three spans, with two identical side spans and a middle span kept at consistent lengths of 22.1 m and 29.5 m, respectively. Characteristics that would otherwise affect the structural response such as the member material properties, deck width, mean pier height, and member cross-section are identical to the baseline bridge. Characteristics such as the slanted length of support piers and abutments are subject to changes in accordance to the variations of skew angles and curvature and other realistic design considerations. The superelevations of the bridges follow the typical values in the AASHTO (2007) design guidelines. The geometries selected for the parametric study are summarized below in Table 3.3.

Bridge #1 is a representation of a regular, straight bridge serving as a benchmark case for comparison purposes. Bridges #2 – 5 were constructed for evaluating independent effects of skew and curvature, as well as studying the effects of the parameter. Bridges #6 – 8 incorporate both skew and curvature, and Bridge #6 serves as the baseline model as described above.

Table 3.3 Bridge Configurations for Parametric Study: Part II

Bridge #	Skew (degrees)	Curvature Radius (m)	Super Elevation (degrees)
1*	0	0	0
2	30	0	0
3	45	0	0
4	0	1370	4
5	0	910	6
6**	30	1370	4
7	45	1370	4
8	30	910	6

Note: * Benchmark model and ** Baseline model

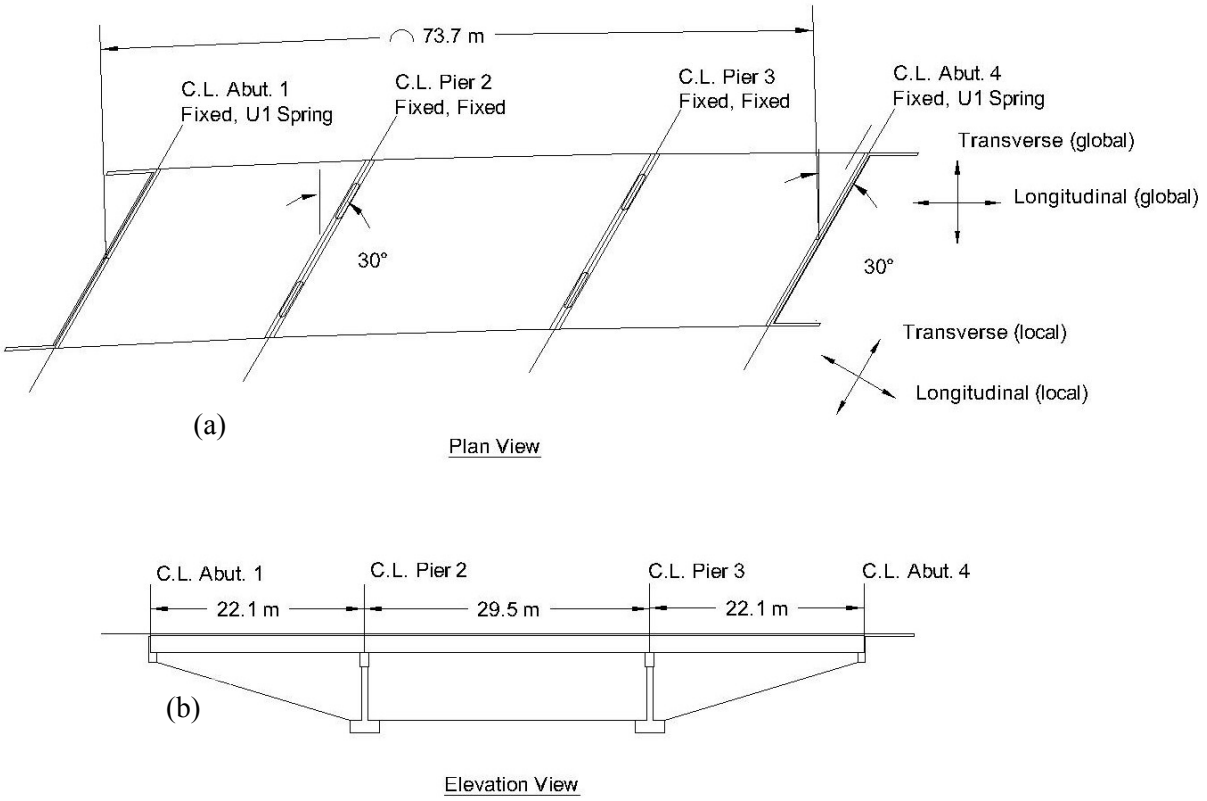

Figure 3.6 (a) Plan View **(b)** Elevation View of Bridge – Radius 1730 m. Skew 300

Modal analysis is conducted on each of the bridge configurations introduced above for the first 3 modes. Ritz vectors are utilized for determining mode shapes, and target dynamic participation ratios are set at 99 % in the local longitudinal and transverse directions. Depictions

of the mode shapes and tabulated summaries of the periods of vibration are given below in Fig. 7 and Table 3.4, respectively.

The benchmark model (#1 in Table 3.3), which has no skew or curvature, has a longitudinal first mode vibration of period of 0.208 sec. Second and third modes of vibration are vertical and torsional at mid spans, respectively (Fig. 3.7). The curved bridge configurations (#4 and #5) have comparable modes and period ranges of vibration as the benchmark bridge. The skewed bridge configurations (#2 and 3) have shorter periods of vibration. The fundamental period of vibration of both skewed bridges (#2 and 3) is 0.18 sec, and demonstrates predominantly longitudinal with some torsional vibration. The combined skewed and curved bridge configurations (#6-8) exhibit longitudinal-torsional mode shape similar to that of the skewed bridges (#2 and 3) with an increased period of vibration.

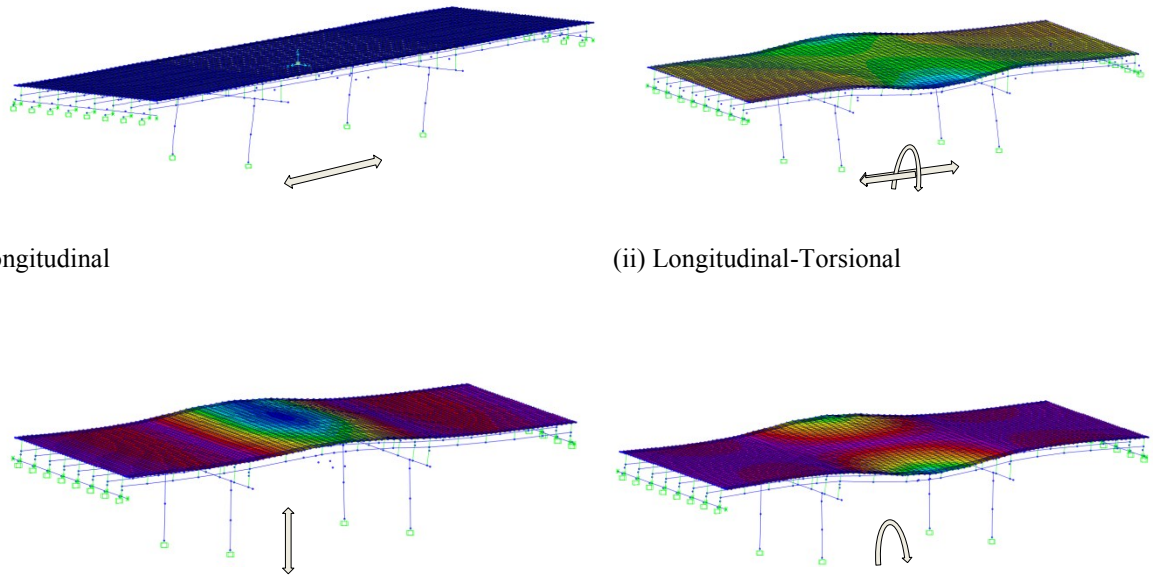

(i) Longitudinal

(ii) Longitudinal-Torsional

(iii) Vertical

(iv) Torsional

Figure 3.7 Mode Shapes

Table 3.4 Bridge Modal Characteristics

Bridge #	Skew (degrees)	Curvature Radius (m)	Mode	Time Period (sec)	Description of Mode Shape
1*	0	0	1	0.21	(i) Longitudinal
			2	0.18	(iii) Vertical
			3	0.18	(iv) Torsional
2	30	0	1	0.18	(ii) Longitudinal – Torsional
			2	0.18	(ii) Vertical
			3	0.17	(iv) Torsional
3	45	0	1	0.18	(ii) Longitudinal – Torsional
			2	0.18	(ii) Vertical
			3	0.16	(iv) Torsional
4	0	1370	1	0.20	(i) Longitudinal
			2	0.18	(iii) Vertical
			3	0.17	(iv) Torsional
5	0	910	1	0.21	(i) Longitudinal
			2	0.18	(iii) Vertical
			3	0.18	(iv) Torsional
6**	30	1370	1	0.20	(ii) Longitudinal – Torsional
			2	0.181	(ii) Vertical
			3	0.17	(iv) Torsional
7	45	1370	1	0.19	(ii) Longitudinal – Torsional
			2	0.17	(ii) Vertical
			3	0.16	(iv) Torsional
8	30	910	1	0.20	(ii) Longitudinal – Torsional
			2	0.20	(ii) Vertical
			3	0.19	(iv) Torsional

Note: * Benchmark model and ** Baseline model

3.5 **Parametric Study Results – Baseline Model**

Evaluation Criteria

The seven time-history load sets described previously are applied to each of the bridge models, which are evaluated at critical locations for actions and deformations. The demand is compared to the component section capacity using demand-deformation relationships based on a fiber model for member sections (CSI 2011). Among the criteria used for assessment, demand/capacity (D/C) ratios are generated for the column section using axial force-uniaxial moment relationships, and represented using an axial force, biaxial moment surface interaction, shown in Fig. 3.8. Using strain relationships for axial forces and moments in any two orthogonal

directions in the horizontal plane, 3-dimensional curves representing the capacity are developed and plotted together to generate a surface. Visual observation of the 3-dimensional surface shows higher strength for the column in the transverse direction and lower strength in the longitudinal direction. The section capacity is also heavily dependent on the axial load; for higher axial loads both directional components positively increase moment capacity to a limit, followed by a reversal of the behavior.

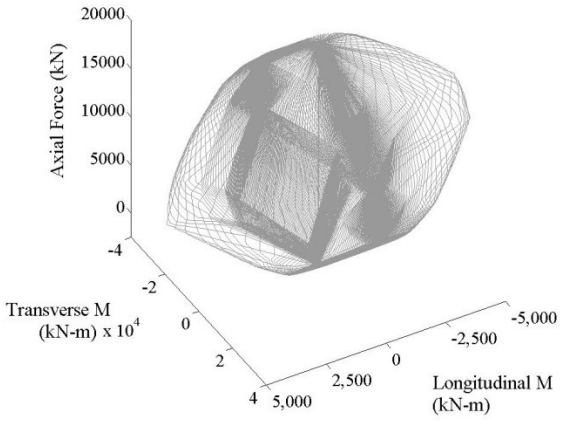

Figure 3.8 Axial Force, Biaxial Moment Interaction Surface for the Pier-column Section

Time-history analysis results of the baseline model

Nonlinear time-history analysis is conducted on the baseline bridge model. Under seven sets of individual earthquake loading, excitation of the bridge at ground supports induces a number of notable structural responses including: longitudinal drift at the top of the piers (Fig. 3.9b); concentrated actions at the column bases (Table 3.2); and resistance provided in the transverse and longitudinal directions. Among the earthquake records, deformations are more notably observed when the bridge is excited by the San Fernando, Loma Prieta, or Kobe earthquake records. The San Fernando earthquake time-history induces the highest demands observed in the substructure, and is therefore used as a basis for evaluation of triaxial capacity against axial and bending forces.

The highest drift ratios in the pier-columns are observed in the top node of the interior, front column (marked in Fig. 3.3), and do not exceed 0.18% and 0.037% in the local longitudinal and transverse directions, respectively (Fig. 3.9b). Resistance of the soil across the back of the abutment ranges from no observed resistance in particular load cases, to 4913.8 kN. The large variance is attributed to the level of deformation induced in the superstructure and the consequent impact on the soil. Under dead load, the bridge is pulled towards the center of mass, and away from the backing soil. If the excitation of the bridge does not cause a large enough deformation to close the gap and induce impact on the soil, no resistance is observed.

Coupling effects in the pier-columns are observed as an effect of the skewed substructure and abutments. Equivalent and critical actions are observed in the interior front and back exterior columns. Although the relative deformation is limited in the superstructure, significant actions develop in the substructure (Table 3.5). Uniaxial analysis shows column shear and moment in the local longitudinal (weak) axis to be controlling. The longitudinal shear induced by the response of the bridge reaches 92.3% of the nominal capacity, while the longitudinal moment reaches 69.2% of its capacity. In addition to the unidirectional analysis, the demand on the critical interior column for the San Fernando earthquake is plotted against the triaxial surface capacity (Fig. 3.9a). The section cut of the triaxial surface shows that the section capacity is exceeded by the demand in several instances of the earthquake excitation, and that subsequent damage or failure may be expected.

Table 3.5 Maximum Demand on Bridge Pier –at Location 1 for the Baseline Bridge (Local Coordinates)

	Axial Force (kN)	Shear (long.) (kN)	Shear (trans.) (kN)	Uniaxial Moment (long.) (kN-m)	Uniaxial Moment (trans.) (kN-m)
Maximum Demand	3872.6	1957.0	706.4	2371.3	9290.3
Demand/Capacity	0.076	0.923	0.289	0.692	0.465

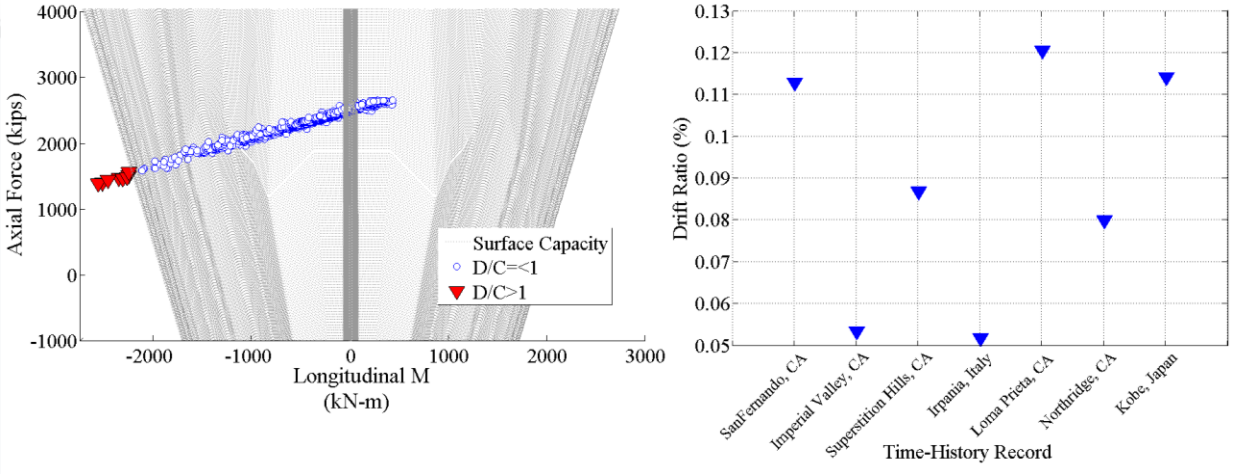

(a) (b)

Figure 3. 9 (a) Triaxial Capacity Demand and **(b)** Drift Ratio - Loma Prieta Time-history

Effect of Earthquake Input Direction

In the analysis of the baseline model above, the earthquake input referred to as the Primarily Longitudinal Combination, is applied fully (100%) in the global longitudinal and partially (40%) in the global transverse direction. In order to make a surface comparison on the effect of earthquake input direction, a new seismic input combination is defined. The new combination consists of a full (100%) load contribution to the global transverse direction and a partial (40%) contribution to the longitudinal direction. This input is referred to as the Primarily Transverse Combination, with which the structural model is reanalyzed.

In comparison to the analysis using the Primarily Longitudinal Combination, the drift ratios at the pier cap for the Primarily Transverse Combination are reduced in the longitudinal and transverse directions (Fig. 3.10a and b). Comparatively, maximum D/C ratios developed in the columns for the Primarily Transverse Combination are also on average 55.5% smaller. This is predominantly attributed to the asymmetrical strength and rigidity of the column sections in the transverse direction, and the added stiffness derived from the transverse fixity at the abutments. The abutment reactions are also lower in all six degrees of freedom for the transverse combination in comparison to the longitudinal combination. The column critical locations do match for both combinations and those critical locations are the focus points for the analyses to follow.

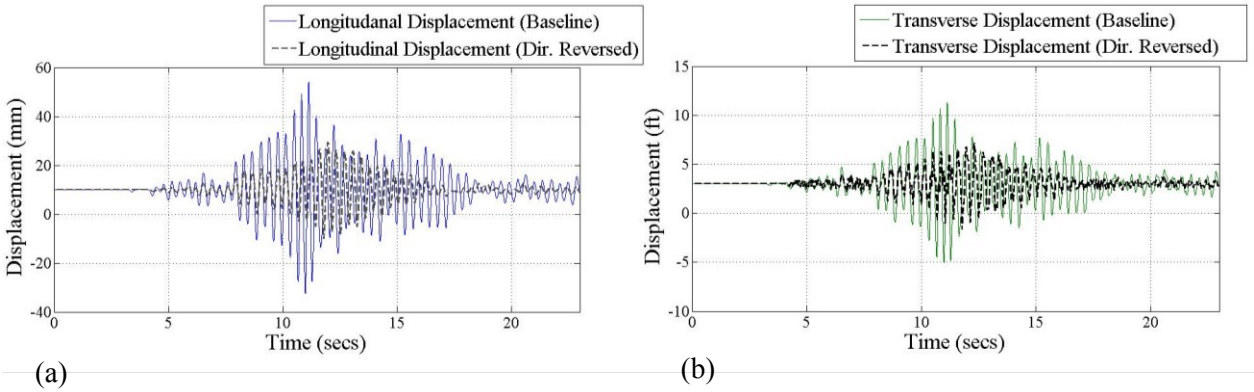

Figure 3. 10 (a) Longitudinal and **(b)** Transverse Drift Ratios of Baseline Bridge with Reversed Input Direction - Top of Pier - Loma Prieta Time-history (Location 1 – Fig. 3.3)

Effect of support condition

Another parameter investigated in this study is the effect of a less rigid abutment support. The analysis showed that small variations in support condition significantly affect the excitation and subsequent distribution of actions in the bridge model. In order to study the effect of imposing an entirely different support condition, the integral abutments are substituted with bearing pads and reinforced with shear keys. The support connection is modeled by restraining

translation in the vertical and transverse directions and rotation about the vertical and longitudinal axes. In addition, a three inch gap spring is used to represent the typical longitudinal expansion allowed between the superstructure and abutment. The results from the analysis show that the use of a bearing type connection releases the structure in the longitudinal direction, increasing the structural period and reducing the structural demand. Modal analysis yields an increased period of 0.394 sec and induces equivalent modes of vibration to the baseline model.

The results of the time-history analyses show that changing the support condition drastically lowers the demand on the piers. The D/C ratios developed at maximum excitation of the bridge structure do not exceed D/C ratios developed under a dead load analysis with no ground motion excitation. In addition the bearing supports develop significantly smaller forces, with transverse force and moment 12.3% and 33.6% lower than those of the integral abutment, respectively. At the pier connection, actions developed across the 6 DOF were 53.7% lower than those of the integral abutment case. This may infer that there are significant advantages to employing bearing type supports at the abutments for curved and skewed bridges. On the other hand, designers should make appropriate considerations to potential pounding effects, as well as the strength of transverse support components such as shear keys, despite it not being a concern for this specific bridge configuration and loading scenario.

3.6 **Parametric Study Results – Curved and Skewed Bridge Configurations**

The analyses described above evaluate the impacts of design considerations for the base line model. In this section, the effects of curvature and skew are further analyzed in a suite of bridge configurations, shown in Table 3.3. The results of the baseline model are used as a reference for comparison of trends, while the bench mark model (no skew or curvature) is used as a control for evaluating geometric effects. The discussion on the bridge responses to seismic loading includes:

drift ratios at the pier cap location (Fig. 3.11); resistance exerted by the backing soil (Fig. 3.12); shear demand developed in the substructure (Figs. 3.13 and 3.14); and D/C ratios due to bending with identification of the respective critical locations in pier-columns (Figs. 3.15 and 3.16).

Critical drift ratios at the top of interior columns

The excitation of the bridges induces relatively low deformation, regardless of geometric configuration (Fig. 3.11). The displacements in both directions are observed to be minimal, with relatively higher longitudinal displacements observed in the primary axis of loading. The bridge configurations are composed of non-slender reinforced concrete members that are connected integrally to abutments and piers. Subsequently, large deformations are not easily incurred without significant damage to members or connections. Behavioral effects observed in the model sets would likely be amplified in less structurally rigid bridges with more flexible supports.

Planar rotation in the substructure is observed in skewed bridges, characterized by higher percentages of translational drift and lower percentages of longitudinal drift, measured at pier caps. Effects from curvature on the bridge translational motion are not observed due to the constraining nature of the abutments. Despite the limited deformation observed, the bridge geometries incorporating skew and curvature result in trends of higher resisting forces in the substructure and abutment.

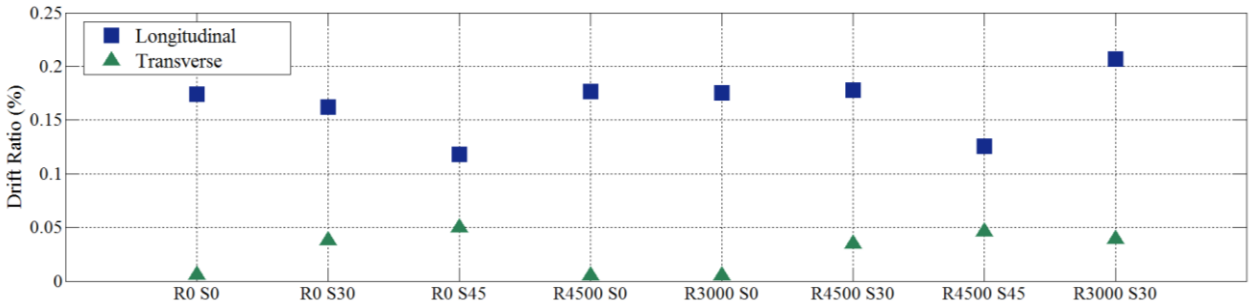

Figure 3. 11 Longitudinal and Transverse Drift Ratio at Pier

Resistance behind integral abutment

The resistance of the soil at the abutment is a function of the induced vibration from effects of geometry, and the resultant displacement in the longitudinal direction. The non-skewed bridge configurations induce primarily longitudinal vibration and therefore, yield the highest resistance from soil springs (Fig. 3.12). Skewed bridges induce more planar rotational motion about the center of the superstructure. This causes substantially higher forces on the transverse supports of the abutments, and less stress longitudinally on the backing soil. Alternative abutment configurations where initial transverse resistances are comparable, such as shear keys or wing walls, would be heavily loaded in the scenarios involving skewed geometries and may exceed expected capacities.

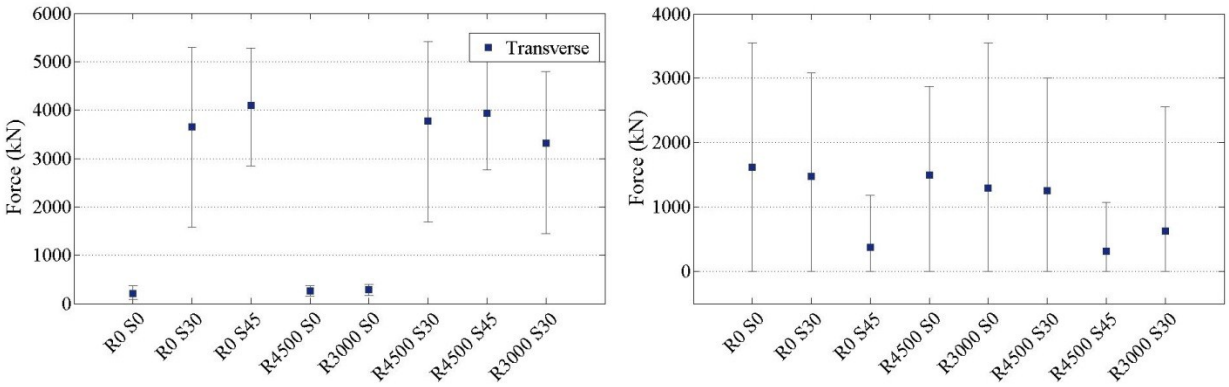

Figure 3. 12 Reaction Force at Abutment – (Global)

Shearing forces in the pier-columns

The shear capacity of the pier-columns was calculated using section 5.8.3.3 (neglecting code based safety factors) of the AASHTO LRFD Bridge Specifications for determination of nominal shear resistance of concrete members (AASHTO, 2007). The shear capacity of the section is heavily dependent on axial, moment and shear demand, thus a comparison of the capacity to the shear loading over the span of the time history is made, as shown in Fig. 3.13. A summary of the critical D/C ratios for each of the configurations is also made, as presented in

Fig. 14. The shear force observed in the substructure of skewed bridges shows significant dependence on the angle of skew. In both skewed bridges, skew causes a reduction in the transverse column shear, and a substantial increase in longitudinal shear. The longitudinal shear in the 45 degree skewed bridge is the highest at 2892 kN, and exceeds the capacity of the section at the two boxed intervals shown in Fig. 3.13. The longitudinal and transverse shear observed in the pier-columns of curved bridges decrease for higher radii of curvature. In the combined geometries, the shearing forces are comparatively higher in the transverse directions and varied in the longitudinal direction. The longitudinal shear forces observed in all the skewed bridge configurations are close to or exceed unity. Significant damage due to longitudinal shear is expected and should be a consideration in design specifically for high angles of skew, and geometries that contain a combination of skew and curvature.

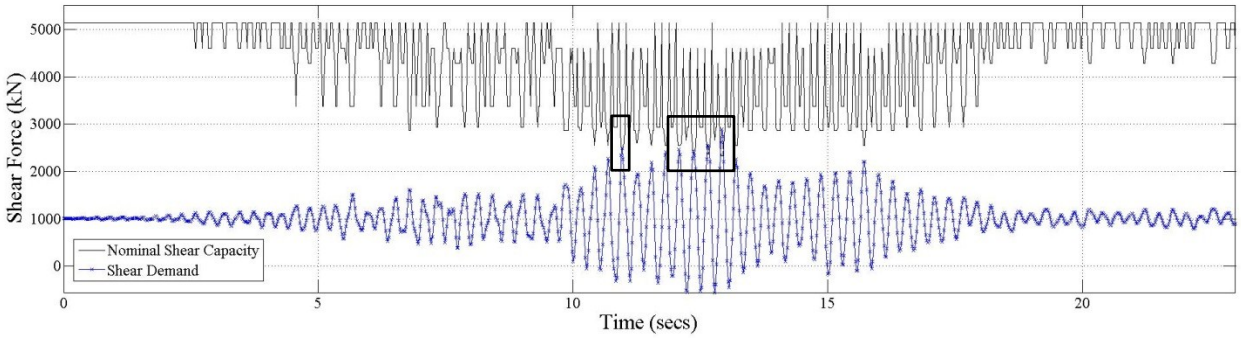

Figure 3.13 Pier Shear Force/ Nominal Capacity – Northridge Time-history

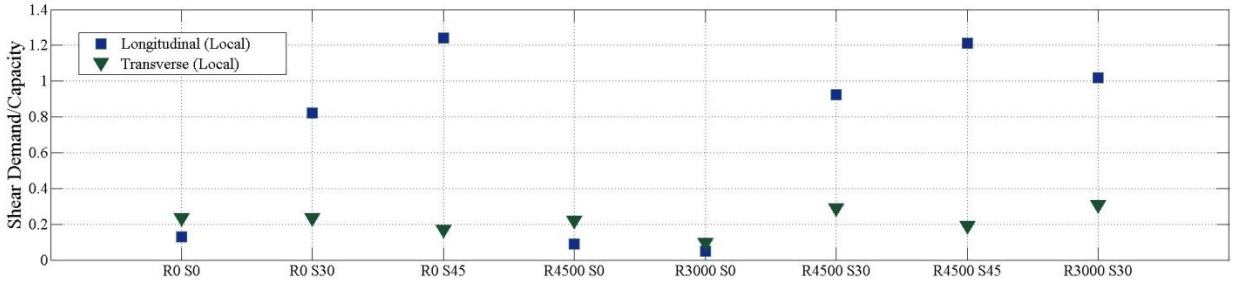

Figure 3. 14 Critical Shear D/C ratios

Axial force and moment demand on pier-columns

In comparison to the benchmark model (of no skew or curvature) the bridge configurations with skew and curvature independently yield higher D/C ratios in the substructure. An evaluation of the pier-columns is conducted first through force-uniaxial moment D/C ratios, then by use of force-biaxial moment surface interaction. The D/C ratios represented in Figs. 3.15a and b are for the time-history and column location yielding the highest demand, although the analysis and discussion is equally accurate for the average behavioral trends. In all model sets, the distribution throughout the pier-columns shows the highest concentration of demand at the bases of pier-columns.

Imposing skew on the bridge structure directs bending in the substructure away from the weak axis of the columns and also causes cross coupling of actions between adjacent columns. In the longitudinal (weak) axis of the pier-columns: the normally critical longitudinal moment decreases proportional to the skew angle (Fig. 3.15a). This is accompanied by an amplification of the moment in the strong axis, which becomes critical in the 45 degree skew configuration. In the curved bridge configurations, although equivalent deformation is observed, longitudinal moment increases proportional to higher degrees of curvature, and is substantially more critical than transverse moments. In the combined geometries, interaction between skew and curvature leads to a stacking effect where higher moments are observed in both the longitudinal and transverse directions. This results in the longitudinal and translational moment reaching 87.9 % and 66.6 % of nominal capacity respectively in combined configurations.

To evaluate the pier-column capacities for axial forces with bidirectional moments, the column demand was evaluated with respect to the force-biaxial moment surface capacity. For each bridge configuration the most critical time-point is selected from the time history, and the

resulting demand is plotted against the triaxial surface capacity (Fig. 3.15b). The plot of the analysis shows the demand exceeding the capacity of the pier-column sections in 3 out of 8 bridge configurations, primarily attributed to moment in the longitudinal moment direction. Significant damage is predicted in the curved bridge configuration of lowest radii (910 m.), due to higher induced longitudinal moment from curvature in combination with induced transverse moment and low axial compression. In the combined curved and skewed bridge configurations, higher longitudinal moments (caused by curvature) combined with higher transverse moment (caused by skew) lead to exceedance of capacity in both 910 m and 1730 m curved, 30-degree skew bridges. Exceedance of capacity does not occur in the 1730 m curved, 45-degree skew bridge configuration due to reduced longitudinal moment attributed to the skew angle. The triaxial analysis performed on the range of geometric configurations illustrates the importance of examining combined loadings, particularly in complex geometries where demands are high in both directions.

Analysis of the different geometries also identifies critical locations for higher seismic demand and locations where damage may occur (Fig. 3.16). For the curved configurations, the two interior columns consistently display higher D/C ratios compared to exterior columns, where the separation is proportionally larger for higher degrees of curvature. For the curved bridge model of highest curvature, this effect leads to exceedance of nominal capacity in interior columns. For skewed bridge configurations, coupling of actions in diagonally opposite pier-columns is observed. Higher force and moment demand in skewed bridges is higher, and focused in front interior and back exterior locations due to coupling and planar rotational. The separations between column sets are also more apparent for higher degrees of skew. The behavior observed in curved and skewed bridges is evident in combined geometries and a

stacking effect is observed. Both skew and curvature have in common the interior front column location as a focus point for high concentrations of demand. This location yields higher shearing forces as well as higher axial and moment demands, which in two of the three combined geometries leads to exceedance of nominal capacity.

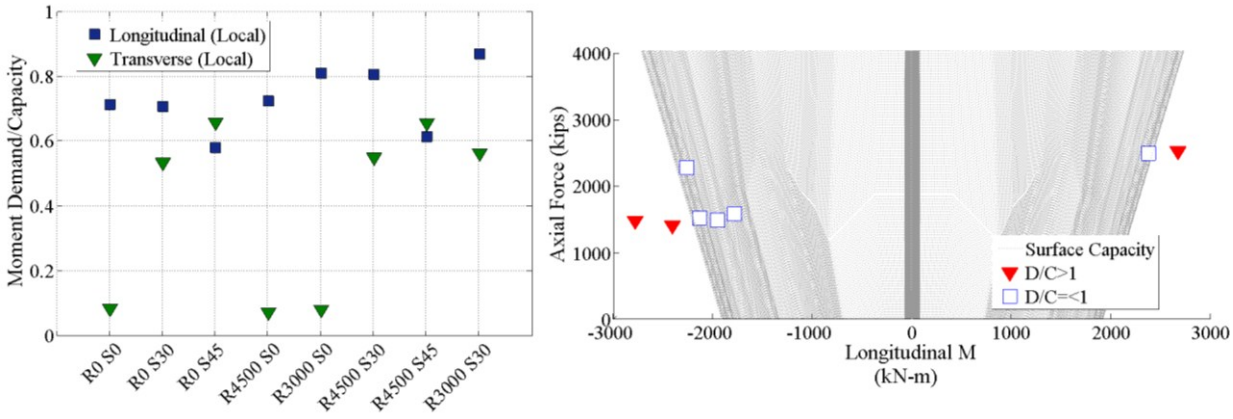

Figure 3.15 (a) Section Analysis – Unidirectional Moment Demand/Nominal Section Capacity at Critical Pier **(b)** Triaxial D/C Ratios of Pier-Columns in Various Bridge Configurations

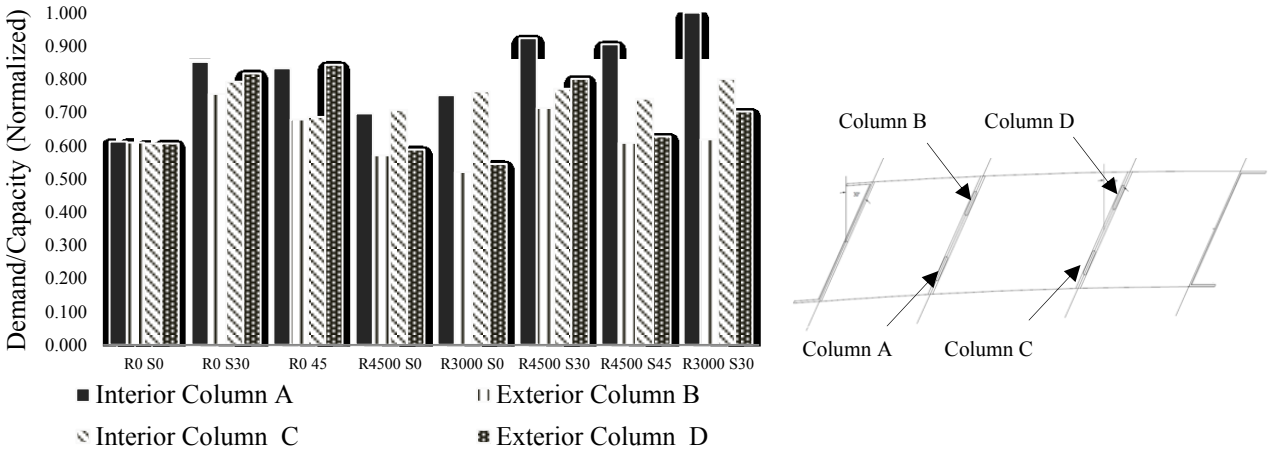

Figure 3.16 Normalized Triaxial Demand Ratios at Critical Pier-Columns

3.7 **Conclusions**

Numerical studies on the seismic performance of bridges that specifically evaluate the combined effects of both curvature and skew were not found in existing studies. There is also limited existing research that focuses specifically on the bridge types designed and built in the Mountain West region. This study examined the seismic behavior of typical, local reinforced

concrete bridges incorporating continuous deck design, integral abutments and stiff backing soils. It also includes the effects of skew and curvature, in various geometric configurations. The study was conducted using non-linear time history analysis on detailed FE models of the bridges. Seven sets of earthquake records scaled to a local Denver, Colorado site location were used in the simulations. Investigations of the effects of earthquake loading direction and abutment support condition were also made. The following conclusions are drawn based on the response of the structural models to ground motions and geometrical and structural component variation:

- Throughout the model sets, the dynamic response of the bridges was found to be fairly rigid in terms of deformation. The superstructure remained essentially elastic and drift ratios observed at column top nodes were limited to 0.2%. Despite limited deformations, actions in the columns of the substructure were found to be critical and exceeded nominal section capacity in several scenarios.
- Ground motion loaded primarily in the global longitudinal direction (100/40) was confirmed to control the design and analysis. Loading shifted to (100/40) in the transverse axes yielded a 55.5% reduction in the column D/C ratios, lower deformations at pier caps, and lower resistances at supports.
- Integral abutments were found to induce substantially higher actions and deformations in the structural model compared to a bearing support. A standard bearing support, if adopted, was found to increase the period of vibration, reduce bridge excitation, and substantially lower the demand on columns, abutments and pier cap connections.
- The effect of skew induced coupling effects between diagonally opposite columns and directed seismic induced actions away from the primary axes. The result exhibits a sharp increase in the observed longitudinal shear and transverse moment in the local axes of the

substructure, supplementing a decrease in longitudinal moment and transverse shear. Higher transverse displacements were observed with larger skew angles, accompanied by lower displacements in the longitudinal direction. The effect of skew was observed to be directly proportional to the skew angle and an established difference was readily visible at the supposed conservative skew level of 30 degrees. The increase in longitudinal shear attributed to skew exceeded the capacity of pier-column members in the 45-degree skew bridges and 30-degree skewed bridges with low radii.

- Curved bridge models induced higher longitudinal moments and overall lower shear demand in the substructure compared to the benchmark model. The interior columns of the bridge with respect to the center of curvature experienced the highest longitudinal moment demand and exceeded the capacity of the member in the analysis of triaxial demand. The demand on the interior, in contrast to exterior, pier-columns was observed to be much higher and increase proportionally to the level of curvature.
- Curved and skewed bridge models exhibited stacking effects proportional to the influence of each geometric parameter. The result is higher observed D/C ratios in the columns, and higher transverse deformation of the superstructure. In some cases stacking effects were observed to counteract each other leading to more conservative behavior than the single geometrical contribution. Bridges incorporating both geometrical components should be evaluated more rigorously, because they develop larger actions in the substructure with concentrations at specific column locations.
- For what is assumed to be a low seismic region, the earthquake loading implemented on the bridge configurations induced actions that exceeded shear and triaxial capacities in the substructure. Although bridges in low seismic regions are generally not considered for

seismic analysis or design, bridges with complex geometric configurations including skew and curvature may need specific seismic analysis as shown in the results of this study.

Acknowledgements

The research study was supported by the Colorado Department of Transportation, which assisted in providing important information and details on current bridge design in the region.

3.8 **References**

AASHTO. (2007). *AASHTO LRFD Bridge Design Specifications* (4th ed.). Washington, DC: AASHTO.

AASHTO. (2009). *AASHTO Guide Specifications for LRFD Seismic Bridge Design* (1st ed.). Washington, DC: AASHTO.

Abdel-Mohti, A., & Pekcan, G. (2008). Seismic Response of Skewed RC Box-Girder Bridges. *Earthquake Engineering and Engineering Vibration*, *7*(4), 415–426.

Abdel-Salam, M., & Heins, C. (1988). Seismic Response of Curved Steel Box Girder Bridges. *Journal of Structural Engineering*, *114*(12), 2790–2800.

Bignell, J. L., LaFave, J. M., & Hawkins, N. M. (2005). Seismic vulnerability assessment of wall pier supported highway bridges using nonlinear pushover analyses. *Engineering Structures*, *27*(14), 2044–2063. doi:10.1016/j.engstruct.2005.06.015

Burdette, N. J., Elnashai, A. S., Lupoi, A., & Sextos, A. G. (2008). Effect of Asynchronous Earthquake Motion on Complex Bridges. I: Methodology and Input Motion. *Journal of Bridge ...*, (April), 158–165.

Button, M., Cronin, C., & Mayes, R. (2002). Effect of vertical motions on seismic response of highway bridges. *Journal of Structural Engineering*, (December), 1551–1564.

California Department of Transportation. (2006). Caltrans Seismic Design Criteria, (1.6), 161.

Computers and Structures Inc. (2011). *CSI Analysis Reference Manual*. Berkeley, California, USA.

Dimitrakopoulos, E. G. (2011). Seismic response analysis of skew bridges with pounding deck–abutment joints. *Engineering Structures*, *33*(3), 813–826. doi:10.1016/j.engstruct.2010.12.004

Earthquake Engineering Research Institute (EERI). (1991). *Costa Rica earthquake of April 22, 1991 : Reconnaissance report. Earthquake Spectra* (Vol. 7, p. 127). Oakland, CA, US.

Earthquake Engineering Research Institute (EERI). (1996). *1994 Northridge Earthquake Reconnaissance Report*. *Earthquake Spectra* (Vol. 11, p. 523).

Galindo, C., Hayashikawa, T., & Julian, D. (2008). Seismic Damage due to Curvature Effect on Curved Highway Viaducts. *jetty.ecn.purdue.edu*.

Galindo, C. M., Hayashikawa, T., & Belda, J. G. (2009). Damage Evaluation of Curved Steel Bridges Upgraded with Isolation Bearings and Unseating Prevention Cable Restrainers, 53–61.

He, X. H., Sheng, X. W., Scanlon, a., Linzell, D. G., & Yu, X. D. (2012). Skewed concrete box girder bridge static and dynamic testing and analysis. *Engineering Structures*, *39*, 38–49. doi:10.1016/j.engstruct.2012.01.016

Itani, A. M., & Pekcan, G. (2011). *Seismic Performance of Steel Plate Girder Bridges with Integral Abutments*. Federal Highway Administration.

Kappos, A. J., Paraskeva, T. S., & Sextos, A. G. (2005). Modal pushover analysis as a means for the seismic assessment of bridge structures. *4th European Workshop on the Seismic Behaviour of Irregular and Complex Structures*. Thessaloniki, Greece.

Kawashima, K., Unjoh, S., & Hoshikuma, J. (2010). Damage of transportation facility due to 2010 Chile Earthquake.

Linzell, D., & Nadakuditi, V. (2011). Parameters influencing seismic response of horizontally curved, steel, I-girder bridges. *Steel and Composite Structures*, *11*(1), 21–38.

Maleki, S, Asce, M., & Bisadi, V. (2006). Orthogonal Effects in Seismic Analysis of Skewed Bridges, (February), 122–130.

Maleki, Shervin. (2002). Deck modeling for seismic analysis of skewed slab-girder bridges. *Engineering Structures*, *24*(10), 1315–1326. doi:10.1016/S0141-0296(02)00066-4

Maragakis, E. (1984). *A model for the rigid body motions of skew bridges*. Pasadena, California.

Mwafy, A. M., & Elnashai, A. S. (2007). Assessment of seismic integrity of multi-span curved bridges in mid-America, (April).

Saadeghvaziri, M. A., Yazdani-Motlagh, A. R., & Rashidi, S. (2000). Effects of soil ± structure interaction on longitudinal seismic response of MSSS bridges. *Soil Dynamics and Earthquake Engineering*, *20*, 231–242.

Seo, J., & Linzell, D. G. (2012). Nonlinear Seismic Response and Parametric Examination of Horizontally Curved Steel Bridges Using 3-D Computational Models. *Journal of Bridge Engineering*. doi:10.1061/(ASCE)BE.1943-5592.0000345

Wakefield, R., & Nazmy, A. (1991). Analysis of seismic failure in skew RC bridge. *Journal of Structural Engineering*, *117*(3), 972–986.

Washington Department of Transportation. (2011). *WSDOT Bridge Design Manual*.

Chapter 4: Effect of Vertical Ground Motion on Complex Reinforced Concrete Bridges

4.1 Introduction

This study presents an assessment of the effect of vertical ground motion on horizontally skewed and curved highway bridges in moderate-to-high seismic regions. Current US seismic bridge design provisions either do not account for effects of vertical ground motion or, as in California, specify a simplistic method for peak ground accelerations larger than 0.6 g. Earthquake ground motion can be subdivided into three primary directional components. Two of these components are in the horizontal plane, at directions perpendicular to each other. The third component is in the vertical direction, typically not considered in the design or analysis of highway bridges per structural code (AASHTO, 2007). When a bridge structure is located at larger distances from active faults, considered far-field, the vertical component attenuates and has less impact on the structural performance as compared to the two horizontal components. For structures in moderate-to-high seismic regions and close proximity to active faults, the vertical component of ground motion is much more prominent and can cause considerable damage to the structure in parallel with the horizontal components. A number of research studies, as reviewed in the following section, have shown the importance of considering vertical ground motion and its contribution to particular modes of failure of reinforced concrete bridges. Previous studies have been mostly limited to bridges with regular geometric configurations. Bridges with complex geometric configurations such as skew and curvature have not yet been rigorously evaluated. Existing studies of curved and skewed bridges subjected to horizontal ground motion have demonstrated that a more involved and often critical response is observed as compared to their regular geometry counterparts. Therefore, it is important to evaluate the performance of

curved and skewed bridges subjected to both horizontal and vertical components of earthquake ground motion to better understand the realistic performance of near-fault bridges.

4.2 **Literature Review**

The vertical component of earthquake ground motion is characterized by compressive P-waves of shorter wavelength, while the horizontal component is characterized by secondary, shear S-waves of longer wavelength. The source spectrum of the vertical component has a lower corner frequency compared to the P-wave spectrum, thus attenuation as waves travel away from the source is more prevalent in the vertical, compared to horizontal, direction. The energy content of vertical ground motion also tends to be less than what is observed in horizontal ground motion over a larger frequency range. In contrast to horizontal ground motion, where energy is distributed through longer periods, the energy in the vertical component tends to be concentrated in a condensed band with short periods (Collier & Elnashai 2001).

The first major investigation into the effect of vertical accelerations on the elastic response of reinforced concrete highway bridges was conducted by Saadeghvariri and Foutch (1991). Three-dimensional finite element (FE) models were constructed of eight 2-span bridges with single and dual bents. Fluctuations in shear capacity resulting from a varying axial force, in addition to reduced energy dissipation capacity in the bents, were attributed to vertical accelerations. Broderick and Elnashai (1995) assessed the failure of a freeway ramp during the 1994 Northridge earthquake using FE models and concluded that static and dynamic analyses utilizing horizontal components only, would not be sufficiently accurate to predict the complete structural behavior and all subsequent failure modes. Collier and Elnashai (2001) concluded that the vertical component of ground motion is significant in near-fault regions, and should be

incorporated into design and analysis for site locations less than 25 km from an earthquake source.

The existing design specifications provide little guidance in terms of an analytical approach to consider vertical ground motion. There is no methodological information available in the AASHTO codes (2007). In the Caltrans Seismic Design Criteria (SDC 2006) an equivalent static load method is employed as an added fraction of the dead load, which is only considered for structures with design peak ground accelerations (PGA) larger than 0.6 g. Vertical P-waves attenuate quickly, as shown in the data presented by Ambraseys and Simpson (ESEE 2001), and for far field site locations the approach employed by structural codes can be conservative. When incorporating vertical ground motion into a seismic analysis, a common approach originally suggested by Newmark et al. (1973), proposes scaling based on a single spectral shape. The spectrum is developed for the horizontal ground motion, and utilizes a 2/3 vertical-to-horizontal (V/H) acceleration ratio to account for vertical effects. For near field site locations however, both approaches can result in underestimation of the effects. This is apparent from the discussion of the frequency content, but it has also been well demonstrated in a large number of studies including, but not limited to Abrahamson and Litehiser (1989) , Bozorgonia and Campbell (2004), Elgamal and He (2008), Kim et al. (2011). Furthermore, Collier and Elnashai (2001) conducted an extensive study where the V/H ratio was confirmed to exceed ratios larger than 1 for fault distances smaller than a 5 km radius from the source of the earthquake, and larger than 2/3 at a 25 km radius depending on the earthquake magnitude.

In addition to seismic contribution of the vertical ground motion component, the arrival time of the horizontal and vertical components of ground motion as well as their relative difference is also considered to be important to the structural response. Silva (1997) demonstrated through

patterned analysis of vertical time histories that short-period vertical ground motion was likely to arrive before subsequent S-waves, while longer-period vertical ground motion arrived at equivalent times. Collier and Elnashai (2001) investigated the difference in arrival time through evaluating two seismic events. The analysis concluded that the time interval at which the waves were separated increased proportional to site distance, with equivalent arrival times observed for site distances less than 5 km from the fault. Kim et al. (2011) found in their investigation of arrival time on RC bridge pier-columns, that the time interval had a relatively minimal effect on the axial and shear demand, but had a rather significant effect on the shear capacity.

4.3 **Prototype Bridge and Earthquake Excitations**

A bridge in a moderate-high seismic region was selected based on its geometric layout and seismic exposure, as to simulate a realistic and representative scenario. The bridge comprises the Pearl St. Overcrossing following State Road 16 located in Tacoma, Washington (hereon referred as the "Tacoma Bridge"). The Tacoma Bridge consists of a 3-span, pre-stressed concrete, box-girder bridge with two sets of three column bents. The bridge is curved at a centerline radius of 436.1 m; the bridge abutments are skewed at 31.72 and 41.725 degrees; and the two bent centerlines are parallel and skewed at 37.7 degrees. A layout of the bridge showing overall dimensions and component cross-sections is shown below in Figure 4.1.

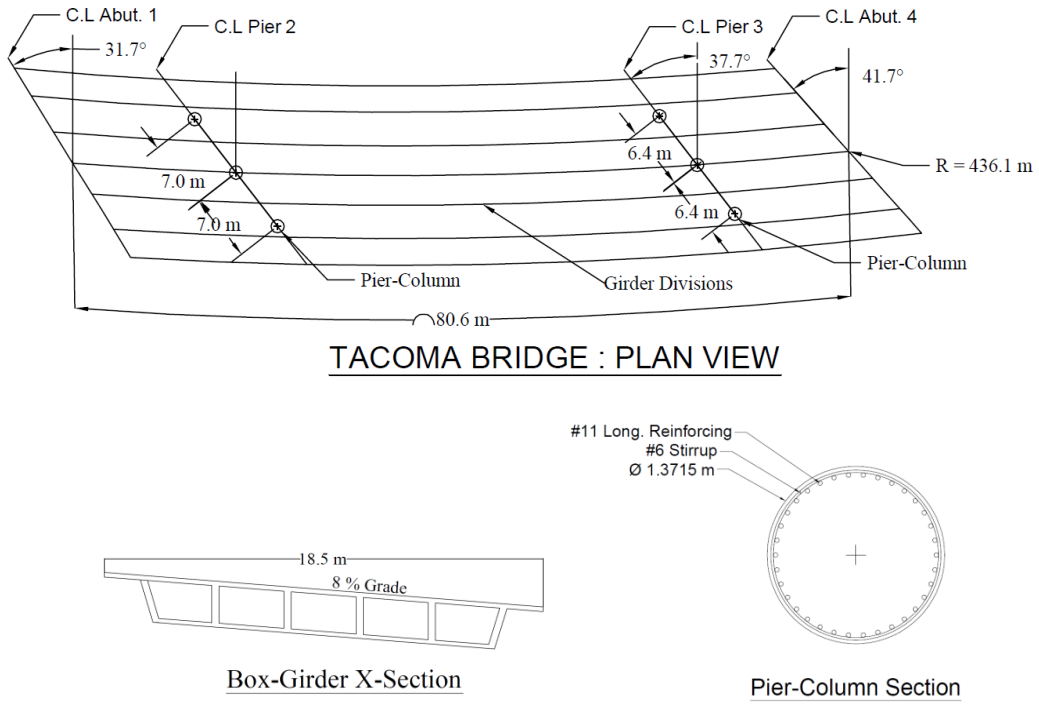

Figure 4.1 Tacoma Bridge Detailing

Structural Modeling

The bridge models were constructed using the finite element software SAP2000 (CSI 2011). The deck is modeled with shell elements, containing both longitudinal and transverse reinforcement. The deck is supported by five box-girders, modeled by line elements and connected to the deck via rigid links. The columns are also represented by line elements and are connected via rigid links and end length offsets. The Tacoma Bridge semi-integral abutment support is modeled using a 2-way rigid support, allowing rotation in all degrees of freedom and translation in the positive vertical and inward longitudinal directions. Although the connection between the deck and roadway is likely to provide some restraint, it is assumed that the connection will be broken in the initial cycles of the earthquake. Geometric and material nonlinearity are included in the numerical analysis, as well as representation of plastic hinging

behavior in the piers. A rendered view of the numerical bridge model is displayed below in Figure 4.2.

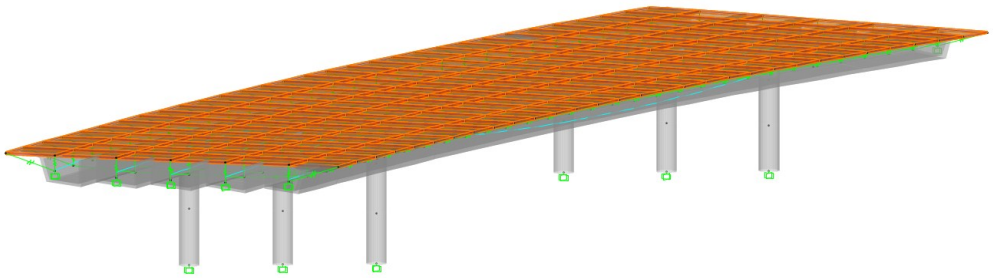

Figure 4.2 Rendered Finite Element Model of the Tacoma Bridge

Ground motion selection and scaling

Twelve sets of vertical and horizontal ground motions were selected from stations for four different moderate-to-high magnitude earthquakes using the Pacific Earthquake Engineering Research (PEER) Center strong motion database. For each earthquake, three different site records were chosen based on vertical peak acceleration, distance to the fault, and PGA V/H ratio. The magnitude of the earthquakes was kept between 6.5 and 7 in moment magnitude (Mw), with variable distances to the rupture plane (D) as shown in Table 4.1. In order to maintain a viable scenario for studying the effects of vertical ground, the distance to the rupture plane does not exceed 15 km.

As discussed previously, the vertical ground motion component attenuates quicker than the horizontal component which indicates that records at further distances from the fault will have lower V/H ratios. This trend is generally observed in ground motion records collected from major earthquake events around the world (Kim et al. 2011), though there are other factors that have equivalent influence such as the site condition and the medium through which the

earthquake travels before reaching the recording station. The records chosen for this study have a scattered correlation between site distance and V/H PGA ratio (Figure 4.3).

The scaling of ground motion, especially when considering the vertical component, is still a topic of widespread debate. Collier and Elnashai (2001) proposed several different procedures for combining vertical and horizontal ground motion, including simplified methods as well as more complex methodologies founded on the coincidence, or otherwise peaks of the directional responses. Scaling all components of ground motion to the design response spectrum has also been conducted (Kunnath et al. 2008). Kim et al. (2011) scaled horizontal motion to the horizontal design response spectrum (DRS), but considered the impact of vertical ground motion through directly altering the V/H acceleration ratios. The approach to the records taken in this study, discussed in the next section, is conducted through use of the Arias Intensity.

A measure often used to quantify the magnitude of an earthquake record is the Arias Intensity (Arias, 1970), which measures the integral of the square of an acceleration time-history. The peak vertical-to-horizontal Arias Intensity ratios for the selected ground motion are shown in Fig. 4.4.

Table 4.1 Characteristics of the Earthquake Records

Event	Year	Mw	Station	D (km)	Vs30 (m/s)	FN (PGA)	V (PGA)	V/H (Arias Intensity)
Northridge	1994	6.69	LA Dam	5.9	629	0.51	0.42	0.54
			Arleta - Nordhoff Fire Station	8.7	298	0.34	0.55	1.37
			Canoga Park	14.7	268	0.42	0.49	0.56
Kobe-Japan	1995	6.9	Takarazuka	0.3	312	0.69	0.43	0.27
			KJMA	1	312	0.82	0.34	0.22
			Nishi-Akashi	7.1	609	0.51	0.37	0.40
Loma Prieta	1989	6.93	LGPC	3.9	478	0.61	0.89	1.16
			BRAN	10.7	376	0.50	0.51	0.52
			Gilroy Array #3	12.8	350	0.56	0.34	0.39
Imperial Valley	1979	6.53	Agrarias	0.7	275	0.37	0.83	5.89
			Holtville Post Office	7.7	203	0.25	0.23	0.69
			Brawley Airport	10.4	209	0.16	0.15	0.90

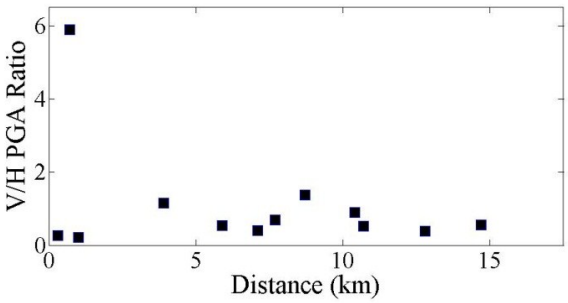

Figure 4.3 Site Distance vs. V/H PGA Ratio

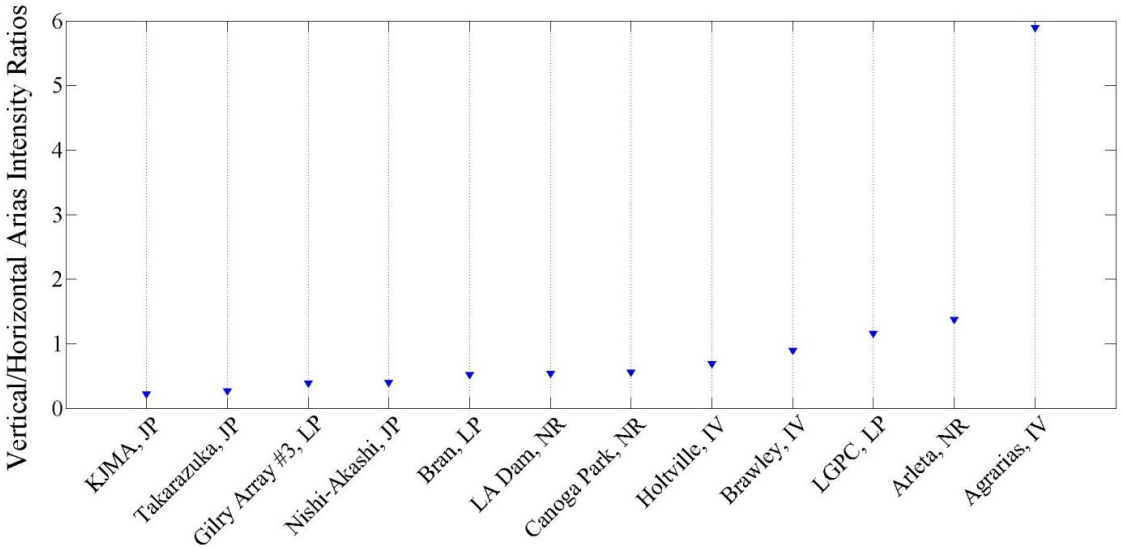

Figure 4.4 Peak V/H Arias Intensity Ratios

The response spectra show the inherent nature of the two different ground motion directions used in this study (Fig. 4.5). The vertical component is more concentrated at higher frequencies, while the horizontal component is more distributed through a larger frequency band. The DRS for horizontal ground motion is developed at the site locations using the AASHTO Guide Specifications for LRFD Seismic Bridge Design (AASHTO 2009). The peak ground acceleration of the DRS developed is 0.33 g, while the max spectral acceleration is 0.72 g. Each earthquake record set consists of a vertical and two horizontal signal components. In the analysis, the fault normal horizontal component is scaled to the DRS developed, while the vertical component is scaled such that the vertical-to-horizontal Arias Intensity ratio remains consistent to the original record. This ensures that the earthquake loading is appropriate for the site condition, while keeping the inherent characteristics of the record and the contribution of the vertical earthquake component consistent.

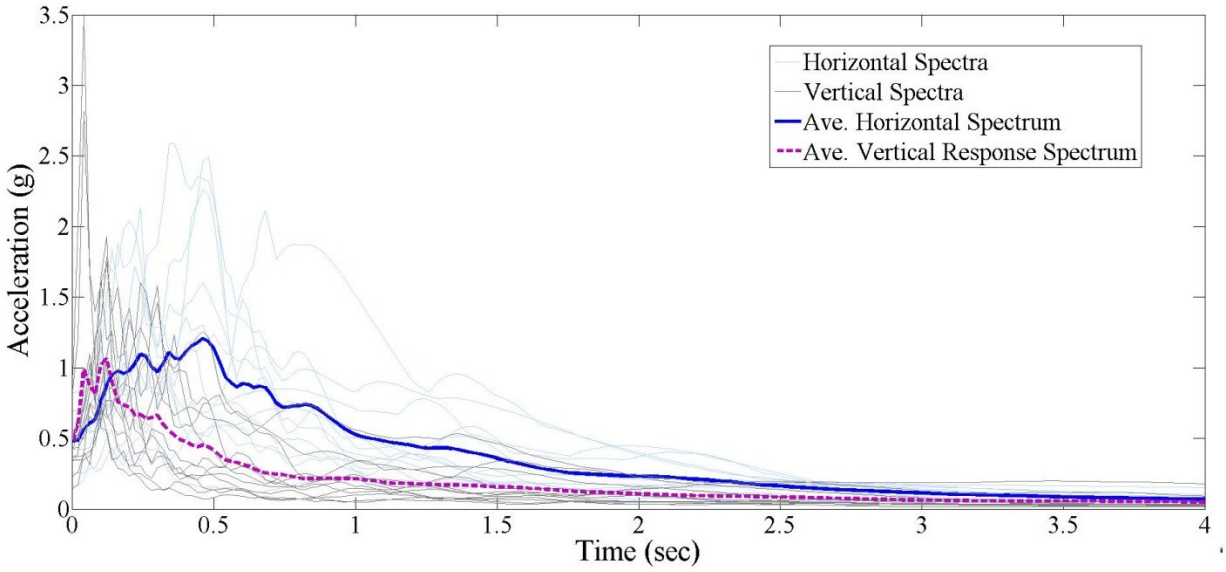

Figure 4.5 Vertical and Horizontal Response Spectra and their Numerical Average

Modal Analysis

Modal analysis is conducted on the Tacoma Bridge, and displayed below are the deformed shapes for the first 3 modes (Fig. 4.6). Ritz vectors were utilized for determining the mode shapes with a target dynamic participation ratio set at 99 % in the local longitudinal and vertical directions. Depictions of the mode shapes and tabulated summaries of the periods of vibration are given below in Fig. 4.6 and Table 4.2, respectively. The Tacoma Bridge exhibits a primarily vertical fundamental mode of vibration with a time period of 0.26 sec. Induced vibration is predominantly vertical at mid span with some torsion towards the interior. Second and third modes of vibration are predominantly transverse and torsional at 0.141 and 0.118 seconds, respectively.

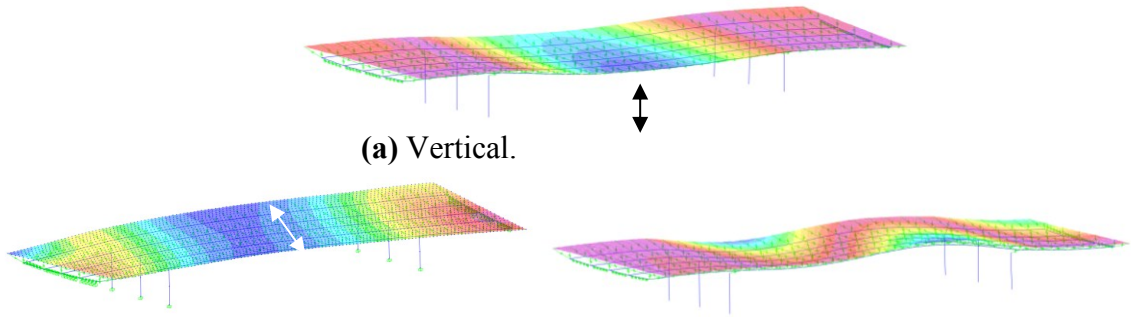

(a) Vertical.

(b) Transverse **(c)** Torsional

Figure 4. 6 Mode Shapes of the Tacoma Bridge (Scaling Factor = 30)

Table 4.2 Modal Characteristics

Mode #	Period (Sec)	Predominant Mode Shape
1	0.263	Vertical
2	0.141	Transverse
3	0.118	Torsional

4.4 **Nonlinear Time-History Analysis Results**

Nonlinear time-history analysis using the direct integration method is conducted. Rayleigh damping coefficients are used to impose 5% damping in the first and second modes of the bridge. The method of time integration follows the Hilber-Hughes-Taylor method with alpha, beta and gamma values of 0.0, 0.25, and 0.5, respectively. The response of the Tacoma Bridge to a single earthquake loading is shown first. The Northridge-Arleta time-history is selected for initial evaluation based on a fault distance of 8.7 km and a PGA V/H ratio of 1.37, representing a case with apparent vertical contribution. The horizontal component of the earthquake is applied in the more critical, longitudinal direction. The response to all earthquake loadings is shown in following sections, and the impact of different vertical ground motion contributions is discussed.

Vertical Time-History Response of the Tacoma Bridge (Northridge-Arleta)

Vertical and horizontal ground motion excitations of the Northridge-Arleta record are applied at the supports of the Tacoma Bridge. The V/H ratio for the record is 1.37, and represents a scenario with strong vertical ground motion contribution. Dynamic analysis yields an induced vibration of the superstructure in the vertical and longitudinal directions, with some deflection in the transverse direction observed at mid span. Due to effects of skew and curvature, torsional vibration at mid-span is also observed at peak excitations about the central longitudinal axis. The torsional motion is shown by the observed differential between the vertical displacements of the exterior and interior edges of the deck (Fig. 4.7a). In contrast, the transverse displacements of the exterior and interior edges of the girders displace in unison, reaching up to 7.4 mm (Fig. 4.7b). The vertical acceleration developed in the deck reaches a peak of 0.5 m/s^2 in the first ten seconds, which may cause disturbance to vehicular traffic (Fig. 4.8).

In the longitudinal direction, the subsequent demand developed in the pier-columns of the substructure increases. It does not induce a significant drift deformation however, and is limited to less than a 1 mm displacement at the top of the column.

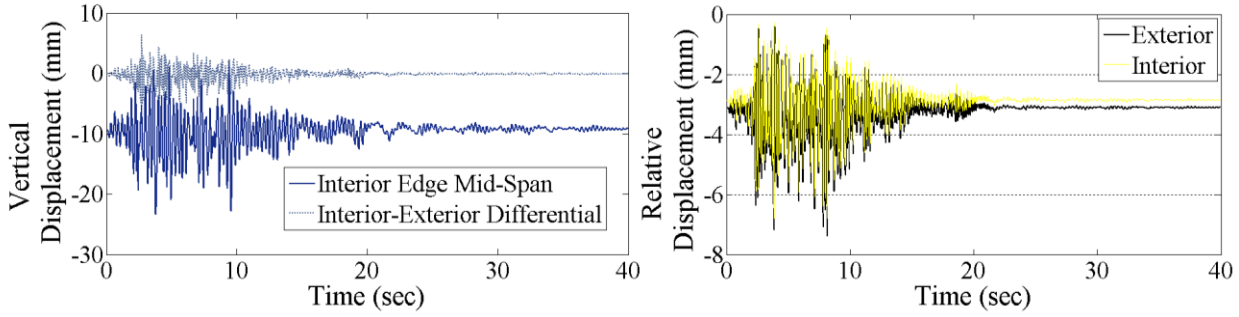

(a) **(b)**

Figure 4.7 (a) Vertical and **(b)** Transverse Displacements of the Deck at Mid-span – Northridge: Arleta

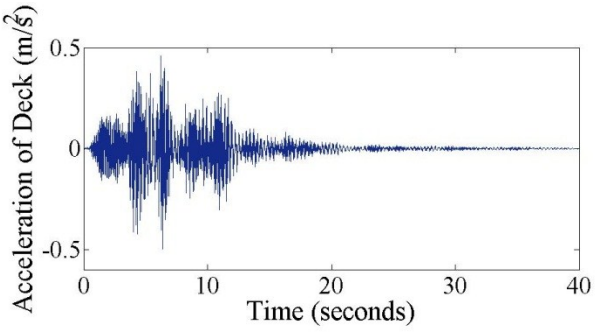

Figure 4. 8 Vertical Acceleration of Deck at Mid-span – Northridge: Arleta

At the substructure, the interior column undergoes the highest longitudinal deformation under the dead weight of the bridge in comparison to the other columns. The center and exterior columns follow with progressively lower initial displacements. Under earthquake ground motion excitation, the interior column is the most rigid and displays the lowest peak displacement in the longitudinal direction. The middle and exterior columns display progressively larger peak displacements, respectively. High axial compressive and tensile strains are observed in all pier-columns, and are amplified by the addition of vertical ground motion. The girders are subjected to large tensile strains as a result of large deformations in the superstructure. At the abutments,

in-plane rotations of the deck, specifically at the exterior edges, is observed and attributed to the overall skewed geometry. Uplift of the superstructure is observed at both abutments, with displacements in the positive vertical direction exceeding up to 24 mm (Fig. 4.9). Uplift is concentrated primarily around the exterior edge of the bridge, which can induce issues of improper loading and weakening of the support system and shear keys.

In comparison to the combined ground motion case (horizontal and vertical) discussed, exclusion of vertical excitation in the second (horizontal only, denoted below as H) diminishes the vertical excitation at mid-span (Fig. 4.9b). This reduces maximum deformation of the substructure, and the axial strains developed in the columns. The uplift observed in the abutments in the combined case is also not observed with horizontal components of ground motion only.

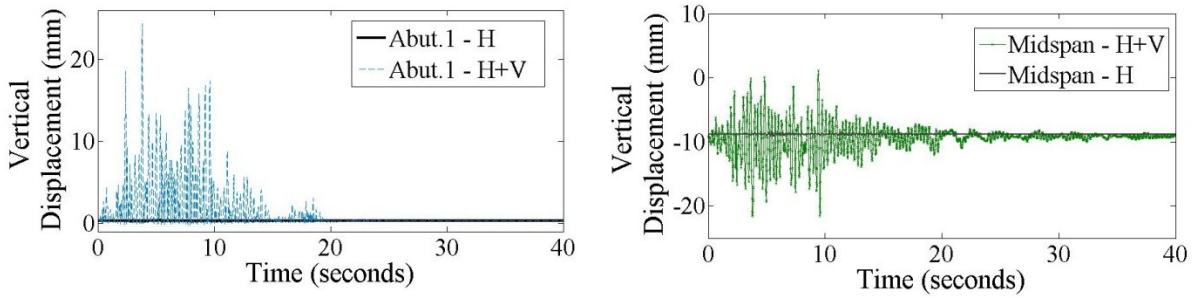

(a) **(b)**

Figure 4. 9 Deformation at **(a)** Abutments and **(b)** Mid-span – Northridge: Arleta

Developed Time-History Actions (Northridge-Arleta)

In bridges that are skewed and curved, the interior column is often a focus point for large stress concentrations and high structural demand. With vertical ground motion the most significant amplifications are observed in the axial forces, and the longitudinal shear and moment developed in the pier-columns (Fig. 4.10). The axial compression forces (Fig. 4.10a) are critical at the bases of the columns and amplify up to 7229 kN and reduce to 828.9 kN. The

amplification and reduction in axial load lead to larger strains induced in the concrete and rebar, and lower resistive capacity in shear, respectively. The maximum moment developed in the longitudinal direction of the column exhibits a peak moment of 3557.9 kN-m in the horizontal only case (Figure 4.10b). When both horizontal and vertical earthquakes are considered, the peak longitudinal moment increases to 4247.5 kN-m, which amounts for a 19.4% increase in demand.

In shear, the axial load and moment often has influence on the member capacity. The shear capacity with and without the contribution of vertical ground acceleration, is evaluated and plotted against the demand (Fig. 4.10c). The critical shear capacity-to-demand ratio (C/D) developed in the two cases are 1.52 and 1.96 for the inclusion and exclusion of vertical ground motion, respectively. As shown in Fig. 4.10c, the shear demand of this particular bridge does not exceed the nominal capacity. However, by considering the vertical earthquake more realistically, the reduced capacity coupled with increased shear demand causes closer convergence of the entities, which could become an issue for some curved and skewed bridges. This indicates the exclusion of vertical ground motion may cause an un-conservative seismic performance assessment, and can control the design in some instances.

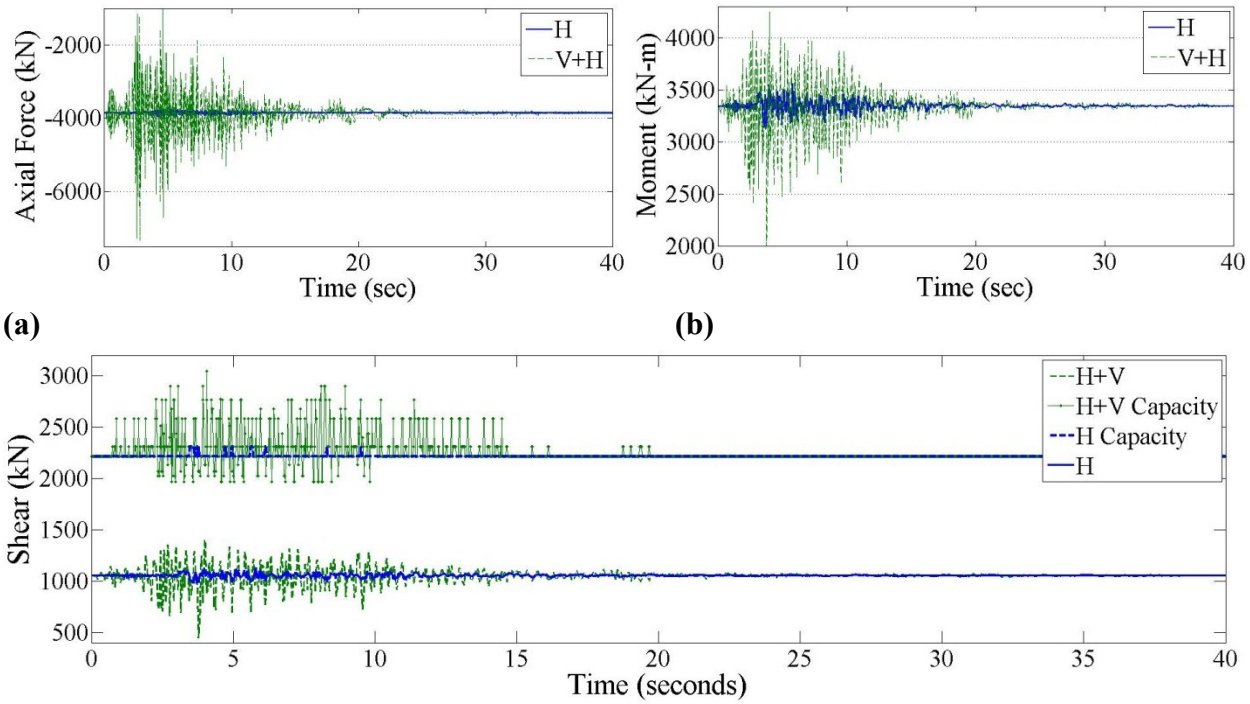

Figure 4.10 Seismic Demand on Interior Colum **(a)** Axial load **(b)** Moment, and **(c)** Shear and Shear Capacity – Northridge Arleta

The capacity of the column section over the course of the earthquake is heavily dependent on the joint effect from the varying axial force and the perpendicular moment demand. The capacity of the column section is therefore evaluated over the full time history through a two-dimensional axial load-moment curve and with a three-dimensional axial load-biaxial moment interaction surface (Fig. 4.11). At the critical demand location for the biaxial moment curve, the C/D ratio is 2.47 and 2.97 for Cases 1 and 2, respectively. Plotting both cases in the tri-axial interaction surface, neither case exceeds capacity, yet the case with vertical ground motion exhibits notably larger demand on the column. The rectangular box on the figure indicates the range of the demand generated for the horizontal ground motion only load case (Fig. 4.11). The marker indicating the critical demand shows the peak demand for the case including vertical ground motion.

The excitation of the superstructure which encompasses most of the seismic mass is primarily resisted by the substructure of the bridge. At the abutments little resistance is provided in the longitudinal directions, and the peak reactions in combined and horizontal load cases do not exceed 40 kN (Fig. 4.12a). The peak vertical reaction force developed under both vertical and horizontal ground is 1425 kN across the abutment, which is amplified from 343.1 kN under dead load conditions (Fig. 4.12b). Uplift of the superstructure from the abutment is also observed, as shown in Fig. 4.9, with excitations reaching 24 mm. This indicates that with vertical ground motion there is additional damage potential from impact (pounding) effects. In comparison to the load case with horizontal ground motion loading only the peak vertical reaction yields a marginal increase to 353.2 kN from dead load.

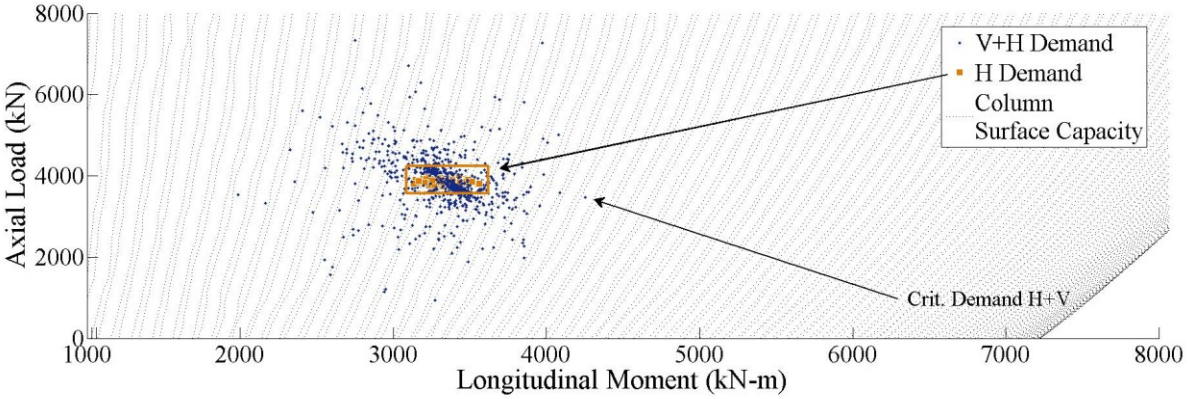

Figure 4. 11 Tri-axial Surface Interaction– Northridge Arleta

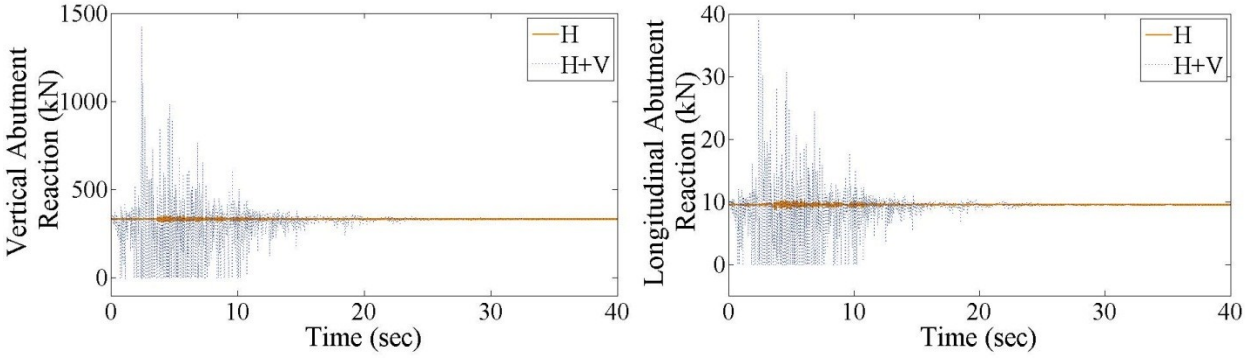

(a) **(b)**

Figure 4. 12 (a) Vertical and **(b)** Longitudinal Abutment Reactions - Northridge Arleta

Response as Function of V/H ratio (all earthquakes)

In the second stage of the analysis, the Tacoma Bridge is subjected to 11 additional ground motions of various vertical component participation ratios. The maximum vertical deformation at mid-span from each load case is recorded and plotted against the corresponding PGA V/H ratio, shown in Figure 4.12a. The PGA V/H ratio as oppose to the Arias Intensity V/H ratio was chosen for cross evaluation since it is a common reference point for researchers and designers alike, and also as an easily identifiable parameter in the ground motion selection stages.

With an increase in the vertical ground motion contribution, the overall structural demand on the bridge increases as a whole. The maximum excitation at the mid-span is observed to increase with a near parabolic behavior. This contributes to a subsequent higher inward deformation observed at columns and abutments. Larger vertical shear forces at abutments are observed, as well as in the girders at the face of the column (Fig. 4.13). Similarly moment demand increases for higher V/H ratios, although the differential grows larger for V/H ratios exceeding one. For V/H ratios smaller than one, nearly no uplift is observed at the abutments. For the latter records, the uplift increases significantly with increasing V/H ratios, at both sides of the abutments. In the most extreme scenarios, we also observe additional uplift at the exterior edge of the compared to the interior. The results for the trends discussed above are plotted in Figure 4.13.

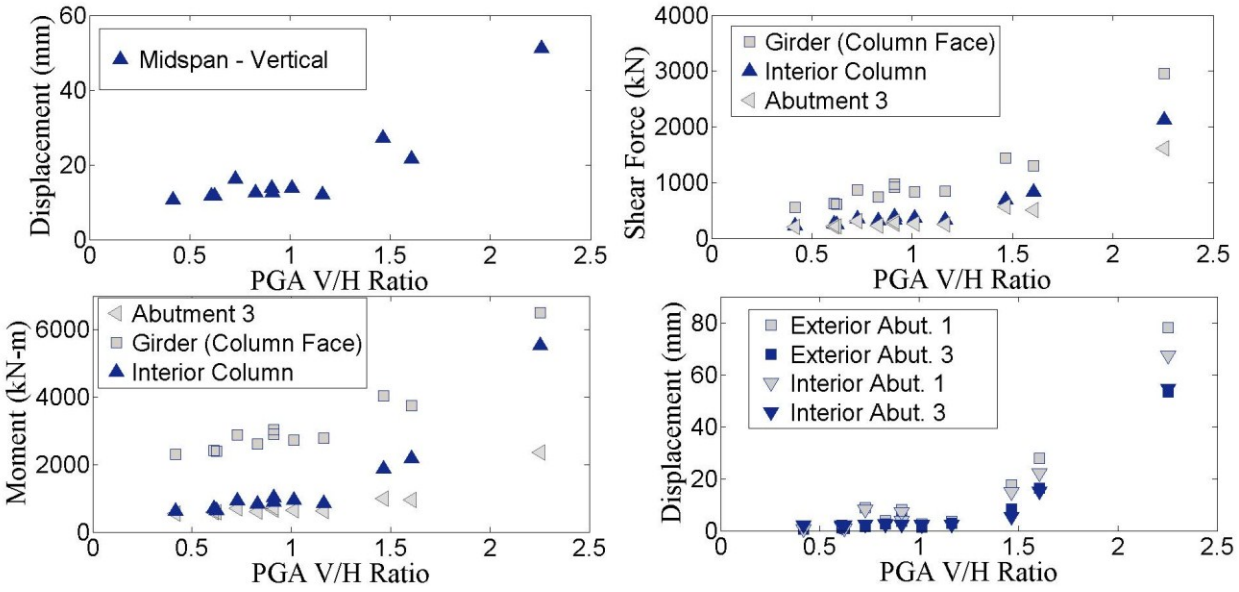

Figure 4.13 Contribution of V/H PGA ratio

A direct comparison between the distance to the fault and the response of the bridge is made across all earthquake records. Although slightly higher V/H PGA ratios are predominantly seen for lower site distances, it is heavily dependent on the site condition, the medium traveled by which the signal traveled, and the characteristics of the signal itself. The trend between V/H ratios and corresponding site distance is therefore scattered. Since the site distance and the V/H ratio are not well correlated, a reasonable range of different V/H ratios should be considered for the near-fault earthquakes in the design in order to capture the critical cases. The numerical analysis performed in this study also suggests that in order to be conservative, the V/H PGA ratio may need to exceed 1 in applicable regions to capture the full contribution of vertical effects.

Effect of Restraining Horizontal and Vertical Abutment

The effects of uplift, and uplift restraint, are investigated through constraining positive vertical, and horizontal inward translation of the superstructure at the abutments. The effects are varied on the response to ground motion. Under dead load in the restrained case, the interior vertical displacement at mid-span is reduced. However under seismic excitation, the relative amplification is much larger in the restrained case. At the abutments, restrained vertical

deformation eliminates the uplift. It imposes concentrated reaction forces however at the interior and exterior locations of up to 2144.6 kN and 4910 kN in the vertical and longitudinal directions, respectively. Comparing the demand on the restrained abutment to the seat type abutment, the resistance forces generated are significantly lower in the latter type abutment. The maximum resistance force generated in the seat type abutment reaches a peak of 1500 kN in the vertical direction, and 50 kN in the longitudinal. However, in the restrained abutment, uplift and pounding effects are eliminated. In the substructure, the additional resistance provided at the abutments reduces the moment and shear demand in the longitudinal direction on interior pier-columns by 42.4% and 54.4%. In the axial and transverse directions of the substructure, seismic demand varies by less than 5%. The load carried by the girders is fairly consistent with the unrestrained case with the exception of the axial compression, which is significantly reduced by up to 42.3 %.

4.5 **Conclusion**

The vertical component of ground motion and it's applicability to seismic design and analysis of bridges has been continually researched since the effects were uncovered. Design codes ignore or simplifying effects of vertical ground motion for the following reasons. Identifying specific failures of past bridges due to vertical ground motion in case studies is difficult, and the range of structures that may be particular susceptible to the effects are narrow and relatively undocumented. The importance of including vertical ground motion in code provisions is shown through the research conducted in this study on skewed and curved, reinforced concrete bridges in the scenarios presented. Based on vertical and horizontal ground motions simulations on numerical models, the following conclusions were made.

- Evaluating the global response of the bridge to ground motion with and without the vertical component of ground motion, the response dictated a significantly higher impact from the ground motion in cases scenarios with larger V/H ratios.
- The deformation observed at mid-span, including torsional effects, was amplified significantly in cases with larger vertical accelerations. The behavior across the twelve earthquakes generated a near parabolic trend, with notable increases in the responses to V/H ratios exceeding unity.
- Significant amplification and reduction of axial forces was observed in the interior columns of the bridge. The subsequent effect on the shear demand and capacity was apparent; however it did not compromise the structural integrity. In the evaluation of the axial force-biaxial moment interaction, a significant increase in the demand from the vertical component of ground motion was observed within the section surface capacity.
- Vertical uplift of the superstructure at the abutments was observed in scenarios involving V/H peak ground accelerations exceeding one. In scenarios involving smaller ratios of vertical-to-horizontal acceleration, no uplift was observed. Cases including uplift generated significantly higher abutment reactions, which may incur issues attributed to pounding effects.
- Restraining uplift and longitudinal deformation of the superstructure at the abutments resulted in significantly higher resistance forces that may exceed typical structural design of abutment components. The benefit however is drastically lowered demand on columns, and axial stresses developed in the superstructure.

- The research conducted pertains to bridges in moderate-high seismic regions. From the modal analysis of the bridge analyzed and the response spectra of the ground motion, it can be seen that the periods of vibration of the bridge and the peak acceleration in the vertical response spectra align. The research may not be pertinent to bridges with longer periods, but may be viable to shorter period bridges. The results also show that vertical ground motion can have considerable effect when the PGA is lower than 0.6g (used in Caltrans), such as the 0.32g design PGA used in this study.
- Comparing V/H Ratios, the most notable responses to vertical ground motion, such as uplift at abutments, amplified deformations at mid span, and increases in structural demand occurred in cases with V/H ratios equal to and larger than one. In the study conducted by Collier and Elnashai (2001), the V/H ratio for many records was found to exceed ratios larger than 1 for fault distances smaller than a 5 km radius from the source of the earthquake, and larger than 2/3 at a 25 km radius depending on the earthquake magnitude.

4.6 **References**

AASHTO. (2007). *AASHTO LRFD Bridge Design Specifications* (4th ed.). Washington, DC: AASHTO.

Abrahamson, N. A., & Litehiser, J. J. (1989). Attenuation of Vertical Peak Acceleration. *Seismological Society of America*.

Arias, A. (1970). A Measure of Earthquake Intensity. *Seismic Design for Nuclear Power Plants*, 438–483.

Bozorgnia, Y., & Campbell, K. W. (2004). the Vertical-To-Horizontal Response Spectral Ratio and Tentative Procedures for Developing Simplified V/H and Vertical Design Spectra. *Journal of Earthquake Engineering*, *8*(2), 175–207. doi:10.1080/13632460409350486

Broderick, B. M., & Elnashai, a. S. (1995). Analysis of the failure of interstate 10 freeway ramp during the Northridge earthquake of 17 January 1994. *Earthquake Engineering & Structural Dynamics*, *24*(2), 189–208. doi:10.1002/eqe.4290240205

California Department of Transportation. (2006). Caltrans Seismic Design Criteria, (1.6), 161. Retrieved from http://www.dot.ca.gov/hq/esc/earthquake_engineering/SDC/

Collier, C. J., & Elnashai, a. S. (2001). a Procedure for Combining Vertical and Horizontal Seismic Action Effects. *Journal of Earthquake Engineering*, *5*(4), 521–539. doi:10.1080/13632460109350404

Computers and Structures Inc. (2011). *CSI Analysis Reference Manual*. Berkeley, California, USA.

Douglas, J. (2001). A comprehensive worldwide summary of strong-motion attenuation relationships for peak ground acceleration and spectral ordinates (1969 to 2000). *Engineering Seismology and Earthquake Engineering*, (01-1).

Elgamal, A., & He, L. (2008). Vertical Earthquake Ground Motion Records: An Overview. *Journal of Earthquake Engineering*, (April 2013), 37–41.

Foutch, D. A., & Saadeghvariri, M. A. (1991). Dynamic Behaviour of R/C Highway Bridges Under the Combined Effect of Vertical and Horizontal Earthquake Motions. *Earthquake Engineering Structural Dynamics*, *20*(6), 535–549. doi:10.1002/eqe.4290200604

Kim, S. J., Holub, C. J., Elnashai, A. S., & Asce, F. (2011). Analytical Assessment of the Effect of Vertical Earthquake Motion on RC Bridge Piers, (February), 252–260.

Kunnath, S. K., Erduran, E., Chai, Y. H., & Yashinsky, M. (2008). Effect of Near-Fault Vertical Ground Motions on Seismic Response of Highway Overcrossings. *Journal of Bridge Engineering*, *13*(3), 282–290. doi:10.1061/(ASCE)1084-0702(2008)13:3(282)

Newmark, N. M., Asce, H. M., & Engrg, C. (2010). Seismic Design Spectra for Nuclear Power Plants. *Atomic Energy*, *99*(PO2), 1973. Retrieved from http://nisee.berkeley.edu/elibrary/Text/S29405

Silva, W. (1997). Characteristics of vertical strong ground motions for applications to engineering design. *FHWA/NCEER Workshop on the Nat'l Representation of Seismic Ground Motion for New and Existing Highway Facilities*, (Technical Report NCEER-97-0010). Retrieved from http://trid.trb.org/view.aspx?id=487442

Chapter 5: Conclusions of the Thesis

Skewed and curved reinforced concrete (RC) highway bridges are an important component of transportation systems. To ensure safe design and construction practices, research is needed to examine the structural behavior of various types of bridge under extreme loading conditions. The research detailed in this study examines the response of skewed and curved bridges of various structural characteristics under seismic loading conditions. In part one, skewed and curved RC bridges are evaluated for a low seismic region. While in part two, a skewed, curved bridge subjected to vertical ground motion is examined for a moderate seismic region. Pertaining to part one of this study a number of conclusions, summarized below, were drawn based on the response of several bridges to earthquake ground motions and geometrical and structural component variation.

The demand imposed by seismic excitation from the low seismic region on skewed and curved bridges causes exceedance of member capacities in the substructures, particularly for more skewed and curved bridges. The usage of integral abutments, in comparison to a pinned abutment, shortened the period of vibration and increased subsequent deformations and stresses developed. Comparing the effects of geometric layout, the effects of skew-caused coupling effects in diagonally opposite columns and directed seismic actions away from primary axes. The result was large amplifications in shear and moment in directions of the columns. In curved bridges, an increase in demand was also developed in the substructure, specifically for the interior column. At the interior column, large longitudinal moments were developed, that in many cases exceeded the column capacity. In the analysis of the combined curved and skew bridges, a stacking effect proportional to the individual influence occurred. The result was higher

observed D/C ratios in the columns, and higher transverse deformation of the superstructure. In some cases stacking effects were observed to counteract each other leading to more conservative behavior than the single geometrical contribution. Bridges incorporating both geometrical components should be evaluated more rigorously, because they develop larger actions in the substructure with concentrations at specific column locations. For what is assumed to be a low seismic region, the earthquake loading implemented on the bridge configurations induced actions that exceeded shear and tri-axial capacities in the substructure. Although bridges in low seismic regions are generally not considered for seismic analysis or design, bridges with complex geometric configurations including skew and curvature may need specific seismic analysis for any earthquake exposure level.

Part two of this study evaluated the impact of the vertical component of ground motion and it's applicability to seismic design and analysis of complex geometry bridges. Application of vertical ground motion has been very limited in design, and is currently not addressed by certain major codes. The effect of vertical ground motion on skewed and curved reinforced concrete bridges is summarized from the analysis and described below.

A model for a skewed and curved RC bridge in a near-fault, high seismic region was developed and subjected to a set of earthquake ground motions with various vertical component contribution. The bridges structural response to ground motion dictated a significantly larger impact from vertical ground motions in higher vertical-to-horizontal peak ground acceleration ratios. In terms of deformation, the vertical component of ground motion led to significantly higher deformations at mid-span, including torsional effects observed about the lengthwise axis. In the substructure, significant amplifications and reductions of the axial forces were developed, particularly for larger vertical-to-horizontal ratios. The shear demand developed in the piers and

effect of axial loads on shear capacity caused closer convergence of the two entities, yet did not compromise the overall structural integrity. In the evaluation of the axial and moment demand, including a triaxial interaction analysis, seismic cases with larger V/H ratios generated larger demand and near exceedance of the column member capacity. Vertical uplift was observed at the abutments in cases with larger V/H PGA ratios, which may induce subsequent pounding effects and damage to abutments. A case with restrained uplift generated significantly larger resistance forces at abutments, but alleviated the demand on the substructure significantly. The research conducted pertains to bridges in moderate-high seismic regions. From the modal analysis performed on the bridge and the response spectra of the ground motion, it can be seen that the periods of vibration of the bridge and the peak acceleration developed in the vertical response spectra align. The research conducted may not be pertinent to bridges with longer periods, but may be viable to design of bridges with shorter. It also shows that vertical ground accelerations can have an impact on bridges in moderate seismic regions with lower peak ground accelerations, and that its exclusion from an analysis may result in a non-conservative design.